A Hierarchy of Models for Inverter-Based Microgrids

Olaoluwapo Ajala, Alejandro D. Domínguez-García, and Peter W. Sauer

Abstract This chapter develops a time resolution based hierarchy of microgrid models that can be utilized in analysis and control design tasks. The focus is on microgrids with distributed generation interfaced via grid-forming inverters. The process of developing the model hierarchy involves two key stages: (1) the formulation of a microgrid high-order model using circuit and control laws, and (2) the systematic reduction of this high-order model to several reduced-order models using singular perturbation techniques. The time-scale based hierarchy of models is comprised of the aforementioned microgrid high-order model (μHOm), along with three reduced-order models (microgrid reduced-order model 1 (μROm1), microgrid reduced-order model 2 (μROm2) and microgrid reduced-order model 3 (μROm3)) which are presented in this chapter. A numerical validation of all the models is also presented.

Olaoluwapo Ajala
Department of Electrical and Computer Engineering, University of Illinois at Urbana Champaign, 306 N Wright St, Urbana, IL 61801 USA, e-mail: ooajala2@ILLINOIS.EDU

Alejandro D. Domínguez-García
Department of Electrical and Computer Engineering, University of Illinois at Urbana Champaign, 306 N Wright St, Urbana, IL 61801 USA, e-mail: aledan@ILLINOIS.EDU

Peter W. Sauer
Department of Electrical and Computer Engineering, University of Illinois at Urbana Champaign, 306 N Wright St, Urbana, IL 61801 USA, e-mail: psauer@ILLINOIS.EDU

The information, data, or work presented herein was supported by the Advanced Research Projects Agency-Energy (ARPA-E), U.S. Department of Energy, within the NODES program, under Award DE-AR0000695; and by the MidAmerica Regional Microgrid Education and Training (MARMET) Consortium, U.S. Department of Energy.

1 Introduction

A microgrid may be defined as a collection of loads and distributed energy resources (DERs), interconnected via an electrical network with a small physical footprint, which is capable of operating in (1) grid-connected mode, as part of a large power system; or (2) islanded mode, as an autonomous power system. The DERs that constitute a microgrid are often interfaced to the electrical network via a grid-feeding inverter, where the output real and reactive powers are controlled to track a given reference; or via a grid-forming inverter, where the output voltage magnitude and frequency are controlled to track a given reference.

As the popularity and adoption of the microgrid concept in electricity systems increases, it becomes necessary to develop comprehensive mathematical models. Models are tools that control engineers, scientists, mathematicians, and other non experts in the field of microgrids, require for the different analysis and control design tasks necessary for development of innovative microgrid technologies. For example, to design and test microgrid frequency controllers, models that capture phenomena in the same time-scale as the frequency, while neglecting phenomena in faster time-scales, are required. Otherwise, the design of such a controller could prove difficult. Accurate mathematical models may be developed for inverter-based microgrids by utilizing concepts from circuit-theoretic and control theory. However, the resulting models are often highly complex and too detailed for the particular application. It therefore becomes necessary to simplify these models to less detailed ones which, though less accurate, can represent the phenomena relevant to the application of interest.

The main contribution of this chapter is the development of a time resolution-based hierarchy of models for inverter-based microgrids. Specifically, the focus is on microgrids with grid-forming-inverter-interfaced power supplies interconnected to loads through an electrical network. Using Kirchhoff's laws and the inverter control laws, a microgrid high-order model (μHOm) is developed. Afterward three reduced-order models (microgrid reduced-order model 1 (μROm1), microgrid reduced-order model 2 (μROm2), and microgrid reduced-order model 3 (μROm3)) are formulated from the μHOm using singular perturbation techniques for model order reduction—the Kuramoto-type model developed in [4] can be extracted from μROm3. The time resolution for which the reduced-order models are valid is also identified, and all four models are explicitly presented with the small parameters used for singular perturbation analysis identified. Finally, a comparison of the model responses, for a given test case, is presented.

The development of high-order and reduced-order models for inverter-based microgrids has received significant attention in the literature recently. More specifically, Pogaku et al. [10] present a high-order model for grid-forming-inverter based microgrids, but exclude a discussion on model-order reduction. Anand and Fernandes [1], and Rasheduzzaman et al. [11] present reduced-order models for microgrids, but the models are obtained using small-signal analysis, which is only valid within certain operating regions. Kodra et al. [5] discuss the model-order reduction of an islanded microgrid using singular perturbation analysis. However, the

electrical network dynamics are not included in the high-order model presented, and a simple linear model, which does not fully capture the dynamics of the islanded microgrid, is used for the singular perturbation analysis. Dörfler and Bullo [4] present a Kuramoto-type model for a grid-forming-inverter developed using singular perturbation analysis. The electrical network is considered in the analysis and sufficient conditions for which the reduced-order Kuramoto-type model is valid are presented. However, the analysis is not as detailed as that presented in this chapter. More specifically, the time-scale resolution associated with the Kuramoto-type is not discussed, the analysis is performed for a lossless electrical network, and the high-order model, on which singular perturbation analysis is performed, is not rigorously developed. Schiffer et al. [13] develop a detailed high-order model for grid-forming-inverter-based microgrids. Singular perturbation analysis is then employed to perform time-scale separation and model-order reduction, as done in this chapter with underlying assumptions stated. However, though the authors claim that the model-order reduction can be performed, the small parameters used for singular perturbation analysis are not explicitly identified, and details of the singular perturbation analysis are not presented. Also, the time resolution associated with the reduced-order model developed is not identified. Luo and Dhople [8] present three models for a grid-forming-inverter-based microgrid, which are obtained by performing successive model reduction steps on a high-order model, using singular perturbation analysis. However, the singular perturbation analysis is presented in a much less detailed form than that in this chapter, the time scales associated with each reduced model are not identified, and the high-order model from which all other models are derived is not explicitly stated with all the small parameters used for singular perturbation analysis identified.

The remainder of this chapter is organized as follows. In Section 2, the relevant concepts, to be used in later developments, are introduced. In Section 3, the microgrid high-order model (μHOm) is developed. In Sections 4–6, by using singular perturbation techniques, we obtain three reduced order models that we refer to as μROm1, μROm2 and μROm3, respectively. Finally, in Section 7, the time resolutions of μROm1, μROm2 and μROm3 are identified, and a comparison between the models responses, for a given test case, is presented.

2 Preliminaries

In this section, we first introduce the $qd0$ transformation of three-phase variables to arbitrary and synchronous reference frames. Next, we introduce graph-theoretic notions used in later developments to develop the network model. Finally, a primer on singular perturbation analysis for time-scale modeling and model-order reduction is presented.

2.1 The $qd0$ Transformation

Let $\alpha(t)$ denote the angular position of a reference frame rotating at an arbitrary angular velocity, $\omega(t)$, and let $\mathbf{f}_{qd0[\alpha(t)]}(t) = \left[f_{q[\alpha(t)]}(t)\ f_{d[\alpha(t)]}(t)\ f_{0[\alpha(t)]}(t)\right]^{\mathrm{T}}$ denote the $qd0$ transform of a vector of 3-phase variables, $\mathbf{f}_{abc}(t) = \left[f_a(t)\ f_b(t)\ f_c(t)\right]^{\mathrm{T}}$, to the reference frame. The general form of the non-power-invariant $qd0$ transformation is given by:

$$\mathbf{f}_{qd0[\alpha(t)]}(t) = \mathbf{K}_1(\alpha(t))\mathbf{f}_{abc}(t), \tag{1}$$

where:

$$\mathbf{K}_1(\alpha(t)) = \frac{2}{3}\begin{bmatrix} \cos(\alpha(t)) & \cos(\alpha(t)-\frac{2\pi}{3}) & \cos(\alpha(t)+\frac{2\pi}{3}) \\ \sin(\alpha(t)) & \sin(\alpha(t)-\frac{2\pi}{3}) & \sin(\alpha(t)+\frac{2\pi}{3}) \\ \frac{1}{2} & \frac{1}{2} & \frac{1}{2} \end{bmatrix},$$

$$\alpha(t) = \int_0^t \omega(\tau)\,d\tau + \alpha(0).$$

The $qd0$ reference frame in Eq. 1 is referred to as the arbitrary reference frame, but when $\alpha(t) = \omega_0 t$, where ω_0 denotes the synchronous frequency, it is referred to as the synchronously rotating reference frame [7].

Assume that $f_a(t)$, $f_b(t)$, and $f_c(t)$ are a balanced three-phase set. Let $\overrightarrow{\mathbf{f}}_{qd0[\omega_0 t]}(t)$ and $\overrightarrow{\mathbf{f}}_{qd0[\alpha(t)]}(t)$ denote the complex representation of $\mathbf{f}_{abc}(t)$ in the synchronously rotating reference frame and the arbitrary reference frame, respectively. Then, by using Eq. 1, we have that for

$$\overrightarrow{\mathbf{f}}_{qd0[\cdot]}(t) := f_{q[\cdot]}(t) - \mathrm{j} f_{d[\cdot]}(t), \tag{2}$$

where j denotes the complex variable, i.e., $\mathrm{j} = \sqrt{-1}$,

$$\overrightarrow{\mathbf{f}}_{qd0[\alpha(t)]}(t) = \overrightarrow{\mathbf{f}}_{qd0[\omega_0 t]}(t)\exp(-\mathrm{j}\delta(t)), \tag{3}$$

with

$$\delta(t) := \alpha(t) - \omega_0 t.$$

[Note that because of the balanced assumption on $f_a(t)$, $f_b(t)$, and $f_c(t)$, $f_{0[\alpha(t)]}(t) = 0$.]

Let $\hat{\mathbf{f}}_{qd0[\alpha(t)]}(t) = \left[f_{q[\alpha(t)]}(t)\ f_{d[\alpha(t)]}(t)\right]^{\mathrm{T}}$, and $\hat{\mathbf{f}}_{qd0[\omega_0 t]}(t) = \left[f_{q[\omega_0 t]}(t)\ f_{d[\omega_0 t]}(t)\right]^{\mathrm{T}}$; then from Eq. 2–Eq. 3, it follows that:

$$\hat{\mathbf{f}}_{qd0[\alpha(t)]}(t) = \mathbf{K}_2(\delta(t))\hat{\mathbf{f}}_{qd0[\omega_0 t]}(t), \tag{4}$$

with

$$\mathbf{K}_2(\delta(t)) = \begin{bmatrix} \cos(\delta(t)) & -\sin(\delta(t)) \\ \sin(\delta(t)) & \cos(\delta(t)) \end{bmatrix},$$

and the evolution of $\delta(t)$ governed by:

$$\frac{d\delta(t)}{dt} = \omega(t) - \omega_0. \tag{5}$$

2.2 Graph-Theoretic Network Model

The topology of the microgrid electrical network can be described by a connected undirected graph, $\mathscr{G} = (\mathscr{V}, \mathscr{E})$, with $\mathscr{V}$ denoting the set of buses in the network, so that $\mathscr{V} := \{1, 2, \ldots, |\mathscr{V}|\}$, and $\mathscr{E} \subset \mathscr{V} \times \mathscr{V}$, so that $\{j,k\} \in \mathscr{E}$ if buses j and k are electrically connected. Choose an arbitrary orientation for each of the elements in $\mathscr{E}$; then we can define an incidence matrix, $M = [m_{ie}] \in \mathbb{R}^{n \times |\mathscr{E}|}$, associated with this orientation as follows:

$$\begin{aligned} m_{ie} &= 1 \quad \text{if edge } e \text{ is directed away from node } i, \\ m_{ie} &= -1 \quad \text{if edge } e \text{ is directed into node } i, \\ m_{ie} &= 0 \quad \text{if edge } e \text{ is not incident on node } i. \end{aligned}$$

Connected to some buses, we assume that there is an inverter-interfaced source, the dynamics of which are described in Section 3.1; and at each bus, we assume there is another element, the dynamics of which are described by a generic dynamical model satisfying some properties, as described in Section 3.3.

Let $\mathscr{V}_{\mathscr{I}} \subseteq \mathscr{V}$ denote the set of buses with an inverter-interfaced source. For $j = 1, 2, \ldots, |\mathscr{V}_{\mathscr{I}}|$, let s_j be used to identify variables associated with the inverter-interfaced source connected to bus j. As a result, we can represent the resistance, inductance and current injection of the source as: $R^{(s_j)}$, $L^{(s_j)}$ and $I^{(s_j)}(t)$, respectively.

For $j = 1, 2, \ldots, |\mathscr{V}|$, let l_j be used to identify variables associated with an element connected to bus j. As a result, we can represent the resistance, inductance and current injection of the element as: $R^{(l_j)}$, $L^{(l_j)}$ and $I^{(l_j)}(t)$, respectively.

For $m = 1, 2, \ldots, |\mathscr{E}|$, let $e_m := \{j,k\}$, $\{j,k\} \in \mathscr{E}$. As a result, we can represent the resistance, inductance and current across a line extending from bus j to bus k as: $R^{(e_m)}$, $L^{(e_m)}$ and $I^{(e_m)}(t)$, respectively.

2.3 A Primer on Singular Perturbation Analysis

Definition 1 (Big O notation). Consider a function $f(\varepsilon)$, defined on some subset of the real numbers. We write $f(\varepsilon) = \mathbf{O}\left(\varepsilon^k\right)$ if and only if there exists a positive real number C, such that:

$$\left|f(\varepsilon)\right| \leq C\varepsilon^k, \text{ as } \varepsilon \to 0.$$

The material in this section follows closely from the developments in ([6], pp. 1–12) and ([3], pp. 7–11). Consider the following two-time-scale dynamical model:

$$\begin{aligned} \dot{\mathbf{x}}(t) &= f\left(\mathbf{x}(t), \mathbf{z}(t), \mathbf{w}(t), \varepsilon\right), & \mathbf{x}(0) &= \mathbf{x}^0, \\ \varepsilon\dot{\mathbf{z}}(t) &= g\left(\mathbf{x}(t), \mathbf{z}(t), \mathbf{w}(t), \varepsilon\right), & \mathbf{z}(0) &= \mathbf{z}^0, \\ \mathbf{0} &= h\left(\mathbf{x}(t), \mathbf{z}(t), \mathbf{w}(t), \varepsilon\right), & \mathbf{w}(0) &= \mathbf{w}^0, \end{aligned} \tag{6}$$

with slow and fast time-scales, t and τ, respectively, where $\tau = \frac{t}{\varepsilon}$, $f(\cdot,\cdot,\cdot,\varepsilon) = \mathbf{O}(1)$, $g(\cdot,\cdot,\cdot,\varepsilon) = \mathbf{O}(1)$, and $h(\cdot,\cdot,\cdot,\varepsilon) = \mathbf{O}(1)$.

Assumption 2.1 *Let the bar ($\bar{}$) and tilde ($\tilde{}$) notations be used to describe the slow t-scale and fast τ-scale variables, respectively.* $\mathbf{x}$, $\mathbf{z}$ *and* $\mathbf{w}$ *can be decoupled to*

$$\begin{aligned} \mathbf{x}(t) &= \bar{\mathbf{x}}(t) + \tilde{\mathbf{x}}(\tau), \\ \mathbf{z}(t) &= \bar{\mathbf{z}}(t) + \tilde{\mathbf{z}}(\tau), \\ \mathbf{w}(t) &= \bar{\mathbf{w}}(t) + \tilde{\mathbf{w}}(\tau), \end{aligned}$$

where

$$\begin{aligned} \bar{\mathbf{x}}(t) &= \bar{\mathbf{x}}_{\mathbf{0}}(t) + \varepsilon\bar{\mathbf{x}}_{\mathbf{1}}(t) + \varepsilon^2\bar{\mathbf{x}}_{\mathbf{2}}(t) + \cdots, \\ \tilde{\mathbf{x}}(\tau) &= \tilde{\mathbf{x}}_{\mathbf{0}}(\tau) + \varepsilon\tilde{\mathbf{x}}_{\mathbf{1}}(\tau) + \varepsilon^2\tilde{\mathbf{x}}_{\mathbf{2}}(\tau) + \cdots, \\ \bar{\mathbf{z}}(t) &= \bar{\mathbf{z}}_{\mathbf{0}}(t) + \varepsilon\bar{\mathbf{z}}_{\mathbf{1}}(t) + \varepsilon^2\bar{\mathbf{z}}_{\mathbf{2}}(t) + \cdots, \\ \tilde{\mathbf{z}}(\tau) &= \tilde{\mathbf{z}}_{\mathbf{0}}(\tau) + \varepsilon\tilde{\mathbf{z}}_{\mathbf{1}}(\tau) + \varepsilon^2\tilde{\mathbf{z}}_{\mathbf{2}}(\tau) + \cdots, \\ \bar{\mathbf{w}}(t) &= \bar{\mathbf{w}}_{\mathbf{0}}(t) + \varepsilon\bar{\mathbf{w}}_{\mathbf{1}}(t) + \varepsilon^2\bar{\mathbf{w}}_{\mathbf{2}}(t) + \cdots, \\ \tilde{\mathbf{w}}(\tau) &= \tilde{\mathbf{w}}_{\mathbf{0}}(\tau) + \varepsilon\tilde{\mathbf{w}}_{\mathbf{1}}(\tau) + \varepsilon^2\tilde{\mathbf{w}}_{\mathbf{2}}(\tau) + \cdots. \end{aligned}$$

The dynamical model in Eq. 6 may be rewritten in terms of t and τ as:

$$\begin{aligned} \dot{\bar{\mathbf{x}}}(t) + \frac{1}{\varepsilon}\frac{d\tilde{\mathbf{x}}(\tau)}{d\tau} &= f\left(\bar{\mathbf{x}}(t) + \tilde{\mathbf{x}}(\tau), \bar{\mathbf{z}}(t) + \tilde{\mathbf{z}}(\tau), \bar{\mathbf{w}}(t) + \tilde{\mathbf{w}}(\tau), \varepsilon\right), \\ \varepsilon\dot{\bar{\mathbf{z}}}(t) + \frac{d\tilde{\mathbf{z}}(\tau)}{d\tau} &= g\left(\bar{\mathbf{x}}(t) + \tilde{\mathbf{x}}(\tau), \bar{\mathbf{z}}(t) + \tilde{\mathbf{z}}(\tau), \bar{\mathbf{w}}(t) + \tilde{\mathbf{w}}(\tau), \varepsilon\right), \\ \mathbf{0} &= h\left(\bar{\mathbf{x}}(t) + \tilde{\mathbf{x}}(\tau), \bar{\mathbf{z}}(t) + \tilde{\mathbf{z}}(\tau), \bar{\mathbf{w}}(t) + \tilde{\mathbf{w}}(\tau), \varepsilon\right), \end{aligned}$$

and by setting $\varepsilon = 0$, it follows that:

$$\begin{aligned}
\frac{d\tilde{\mathbf{x}}_0(\tau)}{d\tau} &= 0,\\
\dot{\bar{\mathbf{x}}}_0(t) &= f\left(\bar{\mathbf{x}}_0(t)+\tilde{\mathbf{x}}_{\mathbf{0}}(\infty),\bar{\mathbf{z}}_0(t)+\tilde{\mathbf{z}}_0(\infty),\bar{\mathbf{w}}_0(t)+\tilde{\mathbf{w}}_0(\infty),0\right),\\
\frac{d\tilde{\mathbf{z}}_0(\tau)}{d\tau} &= g\left(\bar{\mathbf{x}}_0(0)+\tilde{\mathbf{x}}_{\mathbf{0}}(\tau),\bar{\mathbf{z}}_0(0)+\tilde{\mathbf{z}}_0(\tau),\bar{\mathbf{w}}_0(0)+\tilde{\mathbf{w}}_0(\tau),0\right),
\end{aligned}$$

and

$$\begin{aligned}
\mathbf{0} &= h\left(\bar{\mathbf{x}}_0(0)+\tilde{\mathbf{x}}_{\mathbf{0}}(\tau),\bar{\mathbf{z}}_0(0)+\tilde{\mathbf{z}}_0(\tau),\bar{\mathbf{w}}_0(0)+\tilde{\mathbf{w}}_0(\tau),0\right),\\
\mathbf{0} &= h\left(\bar{\mathbf{x}}_0(t)+\tilde{\mathbf{x}}_{\mathbf{0}}(\infty),\bar{\mathbf{z}}_0(t)+\tilde{\mathbf{z}}_0(\infty),\bar{\mathbf{w}}_0(t)+\tilde{\mathbf{w}}_0(\infty),0\right).
\end{aligned} \tag{7}$$

Assumption 2.2 *Equation 7 has distinct real roots, one of which is:*

$$\begin{aligned}
\bar{\mathbf{w}}_0(0)+\tilde{\mathbf{w}}_0(\tau) &= \nu\left(\bar{\mathbf{x}}_0(0)+\tilde{\mathbf{x}}_{\mathbf{0}}(\tau),\bar{\mathbf{z}}_0(0)+\tilde{\mathbf{z}}_0(\tau)\right),\\
\bar{\mathbf{w}}_0(t)+\tilde{\mathbf{w}}_0(\infty) &= \nu\left(\bar{\mathbf{x}}_0(t)+\tilde{\mathbf{x}}_{\mathbf{0}}(\infty),\bar{\mathbf{z}}_0(t)+\tilde{\mathbf{z}}_0(\infty)\right).
\end{aligned}$$

Choosing initial conditions $\tilde{\mathbf{x}}_0(0)=0$ and $\bar{\mathbf{x}}_0(0)=\mathbf{x}^0$, let $\bar{\mathbf{z}}_0(t)=\zeta\left(\bar{\mathbf{x}}_0(t)\right)$ be a root of

$$\mathbf{0} = g\left(\bar{\mathbf{x}}_0(t),\bar{\mathbf{z}}_0(t),\nu\left(\bar{\mathbf{x}}_0(t),\bar{\mathbf{z}}_0(t)\right),0\right). \tag{8}$$

As a result, the two-time-scale dynamical model in Eq. 6 may be expressed in the approximate form:

$$\dot{\bar{\mathbf{x}}}_0(t) = f\left(\bar{\mathbf{x}}_0(t),\zeta(\bar{\mathbf{x}}_0(t)),\nu\left(\bar{\mathbf{x}}_0(t),\zeta(\bar{\mathbf{x}}_0(t))\right),0\right), \tag{9}$$

and

$$\frac{d\tilde{\mathbf{z}}_0(\tau)}{d\tau} = g\left(\mathbf{x}^0,\zeta(\mathbf{x}^0)+\tilde{\mathbf{z}}_0(\tau),\nu(\mathbf{x}^0,\zeta(\mathbf{x}^0)+\tilde{\mathbf{z}}_0(\tau)),0\right), \tag{10}$$

where $\bar{\mathbf{x}}_0(0)=\mathbf{x}^0$ and $\tilde{\mathbf{z}}_0(0)=\mathbf{z}^0-\zeta(\mathbf{x}^0)$

Assumption 2.3 *The equilibrium $\tilde{\mathbf{z}}_0(\tau)=\mathbf{0}$ of Eq. 10 is asymptotically stable in $\mathbf{x}^0$, and $\tilde{\mathbf{z}}_0(0)$ belongs to its domain of attraction.*

Assumption 2.4 *The eigenvalues of $\frac{\partial g}{\partial \mathbf{z}}$ (the Jacobian of Eq. 8) evaluated, for $\varepsilon=0$, along $\bar{\mathbf{x}}_0(t)$, $\bar{\mathbf{z}}_0(t)$, have real parts smaller than a fixed negative number.*

Theorem 1 (Tikhonov's theorem). *Let f and g in Eq. 6 be sufficiently many times continuously differentiable functions of their arguments, and let the root, $\bar{\mathbf{z}}_0(t)=\zeta\left(\bar{\mathbf{x}}_0(t)\right)$ of Eq. 8 be distinct and real, in the domain of interest (it follows from the implicit function theorem that the jacobian of Eq. 8 must be invertible). Then, if assumptions 2.1, 2.2, 2.3 and 2.4 are satisfied, Eq. 6 can be approximated by Eq. 9 and Eq. 10, where*

$$\begin{aligned}\mathbf{x}(t) &= \bar{\mathbf{x}}_0(t) + \mathbf{O}(\varepsilon),\\ \mathbf{z}(t) &= \zeta(\bar{\mathbf{x}}_0(t)) + \tilde{\mathbf{z}}_0(\tau) + \mathbf{O}(\varepsilon),\\ \mathbf{w}(t) &= \nu\left(\bar{\mathbf{x}}_0(t), \zeta(\bar{\mathbf{x}}_0(t)) + \tilde{\mathbf{z}}_0(\tau)\right) + \mathbf{O}(\varepsilon),\end{aligned}$$

and there exists $t_0 > 0$ *such that*

$$\begin{aligned}\mathbf{z}(t) &= \zeta(\bar{\mathbf{x}}_0(t)) + \mathbf{O}(\varepsilon),\\ \mathbf{w}(t) &= \nu\left(\bar{\mathbf{x}}_0(t), \zeta(\bar{\mathbf{x}}_0(t))\right) + \mathbf{O}(\varepsilon),\end{aligned}$$

for all $t > t_0$.

In this work, we refer to the approximate slow component in Eq. 9 as the reduced-order model.

Definition 2 (Time resolution). The time-resolution of the reduced-order model in Eq. 9 is the time it takes the approximate fast component in Eq. 10 to reach the equilibrium $\tilde{\mathbf{z}}_0(\tau) = \mathbf{0}$ from an initial state $\tilde{\mathbf{z}}_0(0) = \mathbf{z}^0 - \zeta(\mathbf{x}^0)$.

3 Microgrid High-Order Model (μHOm)

In this section, basic circuit laws are used in conjunction with notions introduced in Section 2 to develop a High-Order model for a grid-forming-inverter-based AC microgrid operating in islanded mode. First, a model is developed for an inverter-interfaced source, which comprises a battery, a 3-phase inverter, an *LCL* filter, and a voltage magnitude controller model. Next, a three-phase model for the electrical network is developed, along with a generic model for an element (typically a load) connected between each bus and the ground. The Microgrid High-Order Model (μHOm) is developed by combining the inverter-interfaced source model, the network model and the generic element model. In this work, the models developed are expressed using the per-unit representation, to ease analysis in later developments.

3.1 Inverter-Interfaced Source Model

The structure of the inverter-interfaced source adopted in this work is comprised of a 3-phase inverter coupled with a battery, an *LCL* filter, and a voltage magnitude controller. An averaged model, as opposed to a switched model, is used to describe the 3-phase inverter dynamics (see [14], pp. 27–38, for more details).

For the inverter connected to bus j of the microgrid network, let $V_{DC}^{(s_j)}$ denote the dc voltage at the inverter input. Let $U^{(s_j)}(t)$, $E^{(s_j)}(t)$, $\hat{E}^{(s_j)}(t)$ and $V^{(s_j)}(t)$ denote the Pulse Width Modulation (PWM) output voltage of the inverter, the in-

ternal voltage of the inverter, the *LCL* filter capacitor voltage, and the voltage at bus j, in per-unit representation, respectively. Let $\Xi^{(s_j)}(t)$ and $I^{(s_j)}(t)$ denote the inverter output current and the filtered inverter output current, in per-unit representation, respectively, let $\Phi^{(s_j)}(t)$ and $\Gamma^{(s_j)}(t)$ denote the state variables for the voltage and current Proportional-Integral (PI) controllers, in per-unit representation, respectively, let $E_r^{(s_j)}(t)$ denote the voltage magnitude controller reference, in per-unit representation, and let $E_r^{(s_j)}(t) = E_{rq}^{(s_j)}(t) - \mathrm{j}E_{rd}^{(s_j)}(t)$, where $E_{rd}^{(s_j)}(t) = 0$, let $\Xi_r^{(s_j)}(t)$ denote the current controller reference, in per unit representation, and let $\Xi_r^{(s_j)}(t) = \Xi_{rq}^{(s_j)}(t) - \mathrm{j}\xi_{rd}^{(s_j)}(t)$, let $P_f^{(s_j)}(t)$ and $Q_f^{(s_j)}(t)$ denote the filtered real and reactive power measurements, respectively. Then, using the $qd0$ transformation discussed in Section 2, the dynamics of the inverter-interfaced source connected to bus j of the microgrid electrical network can be described by:

At each generator bus $j = 1,2...,|\mathscr{V}_{\mathscr{I}}|$, the dynamics of the connected inverter-interfaced power supply are described by:

$$
\begin{aligned}
D_\omega^{(s_j)}\frac{d\delta^{(s_j)}(t)}{dt} &= P_r^{(s_j)} - P_f^{(s_j)}(t),\\
\frac{1}{\omega_c^{(s_j)}}\frac{dQ_f^{(s_j)}(t)}{dt} &= -Q_f^{(s_j)}(t) + E_{q[\omega_0 t]}^{(s_j)}(t)I_{d[\omega_0 t]}^{(s_j)}(t) - E_{d[\omega_0 t]}^{(s_j)}(t)I_{q[\omega_0 t]}^{(s_j)}(t),\\
\frac{1}{\omega_c^{(s_j)}}\frac{dP_f^{(s_j)}(t)}{dt} &= -P_f^{(s_j)}(t) + E_{q[\omega_0 t]}^{(s_j)}(t)I_{q[\omega_0 t]}^{(s_j)}(t) + E_{d[\omega_0 t]}^{(s_j)}(t)I_{d[\omega_0 t]}^{(s_j)}(t),\\
\frac{L^{(s_j)}}{\omega_0}\frac{dI_{q[\omega_0 t]}^{(s_j)}(t)}{dt} &= -R^{(s_j)}I_{q[\omega_0 t]}^{(s_j)}(t) - L^{(s_j)}I_{d[\omega_0 t]}^{(s_j)}(t) + E_{q[\omega_0 t]}^{(s_j)}(t) - V_{q[\omega_0 t]}^{(l_j)}(t),\\
\frac{L^{(s_j)}}{\omega_0}\frac{dI_{d[\omega_0 t]}^{(s_j)}(t)}{dt} &= L^{(s_j)}I_{q[\omega_0 t]}^{(s_j)}(t) - R^{(s_j)}I_{d[\omega_0 t]}^{(s_j)}(t) + E_{d[\omega_0 t]}^{(s_j)}(t) - V_{d[\omega_0 t]}^{(l_j)}(t),\\
\frac{1}{\omega_0}\frac{d\Phi_{q[\alpha^{(j)}(t)]}^{(s_j)}(t)}{dt} &= -\hat{E}_{q[\omega_0 t]}^{(s_j)}(t)\cos(\delta^{(s_j)}(t)) + \hat{E}_{d[\omega_0 t]}^{(s_j)}(t)\sin(\delta^{(s_j)}(t)) - \hat{R}_0^{(s_j)}\Xi_{q[\alpha^{(j)}(t)]}^{(s_j)}(t)\\
&\quad + \hat{R}_0^{(s_j)}I_{q[\omega_0 t]}^{(s_j)}(t)\cos(\delta^{(s_j)}(t)) - \hat{R}_0^{(s_j)}I_{d[\omega_0 t]}^{(s_j)}(t)\sin(\delta^{(s_j)}(t))\\
&\quad - \frac{1}{D_E^{(s_j)}}Q_f^{(s_j)}(t) + E_0^{(s_j)} + \frac{1}{D_E^{(s_j)}}Q_r^{(s_j)},\\
\frac{1}{\omega_0}\frac{d\Phi_{d[\alpha^{(j)}(t)]}^{(s_j)}(t)}{dt} &= -\hat{E}_{q[\omega_0 t]}^{(s_j)}(t)\sin(\delta^{(s_j)}(t)) - \hat{E}_{d[\omega_0 t]}^{(s_j)}(t)\cos(\delta^{(s_j)}(t)) - \hat{R}_0^{(s_j)}\Xi_{d[\alpha^{(j)}(t)]}^{(s_j)}(t)\\
&\quad + \hat{R}_0^{(s_j)}I_{q[\omega_0 t]}^{(s_j)}(t)\sin(\delta^{(s_j)}(t)) + \hat{R}_0^{(s_j)}I_{d[\omega_0 t]}^{(s_j)}(t)\cos(\delta^{(s_j)}(t)),\\
\frac{C^{(s_j)}}{\omega_0}\frac{d\hat{E}_{q[\omega_0 t]}^{(s_j)}(t)}{dt} &= -I_{q[\omega_0 t]}^{(s_j)}(t) - C^{(s_j)}\hat{E}_{d[\omega_0 t]}^{(s_j)}(t) + \Xi_{q[\alpha^{(j)}(t)]}^{(s_j)}(t)\cos(\delta^{(s_j)}(t))\\
&\quad + \Xi_{d[\alpha^{(j)}(t)]}^{(s_j)}(t)\sin(\delta^{(s_j)}(t)),
\end{aligned}
$$

$$
\begin{aligned}
\frac{C^{(s_j)}}{\omega_0}\frac{d\hat{E}^{(s_j)}_{d[\omega_0 t]}(t)}{dt} &= -I^{(s_j)}_{d[\omega_0 t]}(t) + C^{(s_j)}\hat{E}^{(s_j)}_{q[\omega_0 t]}(t) - \Xi^{(s_j)}_{q[\alpha^{(j)}(t)]}(t)\sin(\delta^{(s_j)}(t)) \\
&\quad + \Xi^{(s_j)}_{d[\alpha^{(j)}(t)]}(t)\cos(\delta^{(s_j)}(t)), \\
\frac{L^{(s_j)}_0}{\omega_0}\frac{d\Xi^{(s_j)}_{q[\alpha^{(j)}(t)]}(t)}{dt} &= K^{(s_j)}_{P\gamma}\left(1+\frac{V^{(s_j)}_{DC}K^{(s_j)}_{P\phi}\hat{R}^{(s_j)}_0}{2}\right)I^{(s_j)}_{q[\omega_0 t]}(t)\cos(\delta^{(s_j)}(t)) \\
&\quad - K^{(s_j)}_{P\gamma}\left(1+\frac{V^{(s_j)}_{DC}K^{(s_j)}_{P\phi}\hat{R}^{(s_j)}_0}{2}\right)I^{(s_j)}_{d[\omega_0 t]}(t)\sin(\delta^{(s_j)}(t)) \\
&\quad - \left(R^{(s_j)}_0 + \frac{V^{(s_j)}_{DC}K^{(s_j)}_{P\gamma}}{2}\left(1+K^{(s_j)}_{P\phi}\hat{R}^{(s_j)}_0\right)\right)\Xi^{(s_j)}_{q[\alpha^{(j)}(t)]}(t) \\
&\quad - \frac{V^{(s_j)}_{DC}K^{(s_j)}_{P\gamma}K^{(s_j)}_{P\phi}}{2}\hat{E}^{(s_j)}_{q[\omega_0 t]}(t)\cos(\delta^{(s_j)}(t)) + \frac{V^{(s_j)}_{DC}K^{(s_j)}_{I\gamma}}{2}\Gamma^{(s_j)}_{q[\alpha^{(j)}(t)]} \\
&\quad + \frac{V^{(s_j)}_{DC}K^{(s_j)}_{P\gamma}K^{(s_j)}_{P\phi}}{2}\hat{E}^{(s_j)}_{d[\omega_0 t]}(t)\sin(\delta^{(s_j)}(t)) + \frac{V^{(s_j)}_{DC}K^{(s_j)}_{P\gamma}K^{(s_j)}_{P\phi}}{2}E^{(s_j)}_0 \\
&\quad + \frac{V^{(s_j)}_{DC}K^{(s_j)}_{P\gamma}K^{(s_j)}_{I\phi}}{2}\Phi^{(s_j)}_{q[\alpha^{(j)}(t)]}(t) + \frac{V^{(s_j)}_{DC}K^{(s_j)}_{P\gamma}K^{(s_j)}_{P\phi}}{2D^{(s_j)}_E}Q^{(s_j)}_r \\
&\quad - \frac{V^{(s_j)}_{DC}K^{(s_j)}_{P\gamma}K^{(s_j)}_{P\phi}}{2D^{(s_j)}_E}Q^{(s_j)}_f(t) + K^{(s_j)}_{P\gamma}C^{(s_j)}\hat{E}^{(s_j)}_{q[\omega_0 t]}(t)\sin(\delta^{(s_j)}(t)) \\
&\quad + \frac{K^{(s_j)}_{P\gamma}C^{(s_j)}}{D^{(s_j)}_{\omega}\omega_0}\left(P^{(s_j)}_r - P^{(s_j)}_f(t)\right)\hat{E}^{(s_j)}_{q[\omega_0 t]}(t)\sin(\delta^{(s_j)}(t)) \\
&\quad + K^{(s_j)}_{P\gamma}C^{(s_j)}\hat{E}^{(s_j)}_{d[\omega_0 t]}(t)\cos(\delta^{(s_j)}(t)) \\
&\quad + \frac{K^{(s_j)}_{P\gamma}C^{(s_j)}}{D^{(s_j)}_{\omega}\omega_0}\left(P^{(s_j)}_r - P^{(s_j)}_f(t)\right)\hat{E}^{(s_j)}_{d[\omega_0 t]}(t)\cos(\delta^{(s_j)}(t)), \\
\frac{L^{(s_j)}_0}{\omega_0}\frac{d\Xi^{(s_j)}_{d[\alpha^{(j)}(t)]}(t)}{dt} &= K^{(s_j)}_{P\gamma}\left(1+\frac{V^{(s_j)}_{DC}K^{(s_j)}_{P\phi}\hat{R}^{(s_j)}_0}{2}\right)I^{(s_j)}_{q[\omega_0 t]}(t)\sin(\delta^{(s_j)}(t)) \\
&\quad + K^{(s_j)}_{P\gamma}\left(1+\frac{V^{(s_j)}_{DC}K^{(s_j)}_{P\phi}\hat{R}^{(s_j)}_0}{2}\right)I^{(s_j)}_{d[\omega_0 t]}(t)\cos(\delta^{(s_j)}(t)) \\
&\quad - \left(R^{(s_j)}_0 + \frac{V^{(s_j)}_{DC}K^{(s_j)}_{P\gamma}}{2}\left(1+K^{(s_j)}_{P\phi}\hat{R}^{(s_j)}_0\right)\right)\Xi^{(s_j)}_{d[\alpha^{(j)}(t)]}(t) \\
&\quad - \frac{V^{(s_j)}_{DC}K^{(s_j)}_{P\gamma}K^{(s_j)}_{P\phi}}{2}\hat{E}^{(s_j)}_{q[\omega_0 t]}(t)\sin(\delta^{(s_j)}(t)) + \frac{V^{(s_j)}_{DC}K^{(s_j)}_{I\gamma}}{2}\Gamma^{(s_j)}_{d[\alpha^{(j)}(t)]} \\
&\quad - \frac{V^{(s_j)}_{DC}K^{(s_j)}_{P\gamma}K^{(s_j)}_{P\phi}}{2}\hat{E}^{(s_j)}_{d[\omega_0 t]}(t)\cos(\delta^{(s_j)}(t))
\end{aligned}
$$

$$
\begin{aligned}
&- \frac{K_{P\gamma}^{(s_j)} C^{(s_j)}}{D_{\omega}^{(s_j)} \omega_0} \left(P_r^{(s_j)} - P_f^{(s_j)}(t) \right) \hat{E}_{q[\omega_0 t]}^{(s_j)}(t) \cos(\delta^{(s_j)}(t)) \\
&+ \frac{K_{P\gamma}^{(s_j)} C^{(s_j)}}{D_{\omega}^{(s_j)} \omega_0} \left(P_r^{(s_j)} - P_f^{(s_j)}(t) \right) \hat{E}_{d[\omega_0 t]}^{(s_j)}(t) \sin(\delta^{(s_j)}(t)) \\
&- K_{P\gamma}^{(s_j)} C^{(s_j)} \hat{E}_{q[\omega_0 t]}^{(s_j)}(t) \cos(\delta^{(s_j)}(t)) \\
&+ K_{P\gamma}^{(s_j)} C^{(s_j)} \hat{E}_{d[\omega_0 t]}^{(s_j)}(t) \sin(\delta^{(s_j)}(t)) \\
&+ \frac{V_{DC}^{(s_j)} K_{P\gamma}^{(s_j)} K_{I\phi}^{(s_j)}}{2} \Phi_{d[\alpha^{(j)}(t)]}^{(s_j)}(t),
\end{aligned}
$$

$$
\begin{aligned}
\frac{1}{\omega_0} \frac{d\Gamma_{q[\alpha^{(j)}(t)]}^{(s_j)}(t)}{dt} = &\left(\frac{2}{V_{DC}^{(s_j)}} + K_{P\phi}^{(s_j)} \hat{R}_0^{(s_j)} \right) I_{q[\omega_0 t]}^{(s_j)}(t) \cos(\delta^{(s_j)}(t)) \\
&- \left(\frac{2}{V_{DC}^{(s_j)}} + K_{P\phi}^{(s_j)} \hat{R}_0^{(s_j)} \right) I_{d[\omega_0 t]}^{(s_j)}(t) \sin(\delta^{(s_j)}(t)) + K_{P\phi}^{(s_j)} E_0^{(s_j)} \\
&- K_{P\phi}^{(s_j)} \hat{E}_{q[\omega_0 t]}^{(s_j)}(t) \cos(\delta^{(s_j)}(t)) + K_{P\phi}^{(s_j)} \hat{E}_{d[\omega_0 t]}^{(s_j)}(t) \sin(\delta^{(s_j)}(t)) \\
&- \left(1 + K_{P\phi}^{(s_j)} \hat{R}_0^{(s_j)} \right) \Xi_{q[\alpha^{(j)}(t)]}^{(s_j)}(t) + \frac{K_{P\phi}^{(s_j)}}{D_E^{(s_j)}} \left(Q_r^{(s_j)} - Q_f^{(s_j)}(t) \right) \\
&+ \frac{2C^{(s_j)}}{V_{DC}^{(s_j)}} \left(P_r^{(s_j)} - P_f^{(s_j)}(t) \right) \hat{E}_{q[\omega_0 t]}^{(s_j)}(t) \sin(\delta^{(s_j)}(t)) \\
&+ \frac{2C^{(s_j)}}{V_{DC}^{(s_j)} D_{\omega}^{(s_j)} \omega_0} \left(P_r^{(s_j)} - P_f^{(s_j)}(t) \right) \hat{E}_{q[\omega_0 t]}^{(s_j)}(t) \sin(\delta^{(s_j)}(t)) \\
&+ \frac{2C^{(s_j)}}{V_{DC}^{(s_j)}} \left(P_r^{(s_j)} - P_f^{(s_j)}(t) \right) \hat{E}_{q[\omega_0 t]}^{(s_j)}(t) \sin(\delta^{(s_j)}(t)) \\
&+ \frac{2C^{(s_j)}}{V_{DC}^{(s_j)} D_{\omega}^{(s_j)} \omega_0} \left(P_r^{(s_j)} - P_f^{(s_j)}(t) \right) \hat{E}_{d[\omega_0 t]}^{(s_j)}(t) \cos(\delta^{(s_j)}(t)) \\
&+ K_{I\phi}^{(s_j)} \Phi_{q[\alpha^{(j)}(t)]}^{(s_j)}(t),
\end{aligned}
$$

$$
\begin{aligned}
\frac{1}{\omega_0} \frac{d\Gamma_{d[\alpha^{(j)}(t)]}^{(s_j)}(t)}{dt} = &\left(\frac{2}{V_{DC}^{(s_j)}} + K_{P\phi}^{(s_j)} \hat{R}_0^{(s_j)} \right) I_{q[\omega_0 t]}^{(s_j)}(t) \sin(\delta^{(s_j)}(t)) \\
&+ \left(\frac{2}{V_{DC}^{(s_j)}} + K_{P\phi}^{(s_j)} \hat{R}_0^{(s_j)} \right) I_{d[\omega_0 t]}^{(s_j)}(t) \cos(\delta^{(s_j)}(t)) \\
&- K_{P\phi}^{(s_j)} \hat{E}_{q[\omega_0 t]}^{(s_j)}(t) \sin(\delta^{(s_j)}(t)) - K_{P\phi}^{(s_j)} \hat{E}_{d[\omega_0 t]}^{(s_j)}(t) \cos(\delta^{(s_j)}(t)) \\
&- \left(1 + K_{P\phi}^{(s_j)} \hat{R}_0^{(s_j)} \right) \Xi_{d[\alpha^{(j)}(t)]}^{(s_j)}(t) + K_{I\phi}^{(s_j)} \Phi_{d[\alpha^{(j)}(t)]}^{(s_j)}(t)
\end{aligned}
$$

$$
\begin{aligned}
&- \frac{2C^{(s_j)}}{V_{DC}^{(s_j)}} \hat{E}_{q[\omega_0 t]}^{(s_j)}(t)\cos(\delta^{(s_j)}(t)) + \frac{2C^{(s_j)}}{V_{DC}^{(s_j)}} \hat{E}_{d[\omega_0 t]}^{(s_j)}(t)\sin(\delta^{(s_j)}(t)) \\
&- \frac{2C^{(s_j)}}{V_{DC}^{(s_j)} D_{\omega}^{(s_j)} \omega_0} \left(P_r^{(s_j)} - P_f^{(s_j)}(t) \right) \hat{E}_{q[\omega_0 t]}^{(s_j)}(t)\cos(\delta^{(s_j)}(t)) \\
&+ \frac{2C^{(s_j)}}{V_{DC}^{(s_j)} D_{\omega}^{(s_j)} \omega_0} \left(P_r^{(s_j)} - P_f^{(s_j)}(t) \right) \hat{E}_{d[\omega_0 t]}^{(s_j)}(t)\sin(\delta^{(s_j)}(t)), \\
E_{q[\omega_0 t]}^{(s_j)}(t) = &- \hat{R}_0^{(s_j)} I_{q[\omega_0 t]}^{(s_j)}(t) + \hat{R}_0^{(s_j)} \Xi_{q[\alpha^{(j)}(t)]}^{(s_j)}(t)\cos(\delta^{(s_j)}(t)) \\
&+ \hat{R}_0^{(s_j)} \Xi_{d[\alpha^{(j)}(t)]}^{(s_j)}(t)\sin(\delta^{(s_j)}(t)) + \hat{E}_{q[\omega_0 t]}^{(s_j)}(t), \\
E_{d[\omega_0 t]}^{(s_j)}(t) = &- \hat{R}_0^{(s_j)} I_{d[\omega_0 t]}^{(s_j)}(t) - \hat{R}_0^{(s_j)} \Xi_{q[\alpha^{(j)}(t)]}^{(s_j)}(t)\sin(\delta^{(s_j)}(t)) \\
&+ \hat{R}_0^{(s_j)} \Xi_{d[\alpha^{(j)}(t)]}^{(s_j)}(t)\cos(\delta^{(s_j)}(t)) + \hat{E}_{d[\omega_0 t]}^{(s_j)}(t).
\end{aligned}
$$

where $L_0^{(s_j)}$, $L^{(s_j)}$ and $C^{(s_j)}$ denote the inductances and capacitance of the *LCL* filter, in per-unit representation, respectively; $R_0^{(s_j)}$, $\hat{R}_0^{(s_j)}$ and $R^{(s_j)}$ denote the inverter and filter resistances, in per-unit representation, respectively; $K_{P\phi}^{(s_j)}$ and $K_{P\gamma}^{(s_j)}$ denote the proportional controller gains for the voltage and current controllers, in per-unit representation, respectively, and $K_{I\phi}^{(s_j)}$ and $K_{I\gamma}^{(s_j)}$ denote the corresponding integral controller gains; $D_E^{(s_j)}$ and $D_{\omega}^{(s_j)}$ denote the voltage and frequency droop coefficients, respectively; $E_0^{(s_j)}$ denotes the voltage droop law constant; $\omega_c^{(s_j)}$ denotes the filter cut-off frequency; $P_r^{(s_j)}$ and $Q_r^{(s_j)}$ denote real and reactive power set-points, respectively. See [9], pp. 10–13 for details of this result.

3.2 Network Model

Assumption 3.1 *All lines connecting the network buses can be represented using the short transmission line model [2].*

Let $V_{q[\omega_0 t]}^{(l_j)}(t) - \mathrm{j}V_{d[\omega_0 t]}^{(l_j)}(t)$ denote the per-unit voltage at bus j, and let $R^{(e_m)}$, $L^{(e_m)}$ and $I_{q[\omega_0 t]}^{(e_m)}(t) - \mathrm{j}I_{d[\omega_0 t]}^{(e_m)}(t)$ denote the per-unit resistance, inductance and current across line (j,k), respectively, as introduced in Section 2.2. Then, the voltage across a line connecting bus j and bus k of the network can be described by:

$$
\begin{aligned}
V_{q[\omega_0 t]}^{(l_j)}(t) - V_{q[\omega_0 t]}^{(l_k)}(t) &= \frac{L^{(e_m)}}{\omega_0} \frac{dI_{q[\omega_0 t]}^{(e_m)}(t)}{dt} + R^{(e_m)} I_{q[\omega_0 t]}^{(e_m)}(t) + L^{(e_m)} I_{d[\omega_0 t]}^{(e_m)}(t), \\
V_{d[\omega_0 t]}^{(l_j)}(t) - V_{d[\omega_0 t]}^{(l_k)}(t) &= \frac{L^{(e_m)}}{\omega_0} \frac{dI_{d[\omega_0 t]}^{(e_m)}(t)}{dt} + R^{(e_m)} I_{d[\omega_0 t]}^{(e_m)}(t) - L^{(e_m)} I_{q[\omega_0 t]}^{(e_m)}(t).
\end{aligned}
$$

Let

$$\begin{aligned}
\mathbf{V}^{(\mathscr{V})}_{q[\omega_0 t]}(t) &= \left[V^{(l_1)}_{q[\omega_0 t]}(t)\ V^{(l_2)}_{q[\omega_0 t]}(t)\ \cdots\ V^{(l_{|\mathscr{V}|})}_{q[\omega_0 t]}(t)\right]^{\mathrm{T}},\\
\mathbf{V}^{(\mathscr{V})}_{d[\omega_0 t]}(t) &= \left[V^{(l_1)}_{d[\omega_0 t]}(t)\ V^{(l_2)}_{d[\omega_0 t]}(t)\ \cdots\ V^{(l_{|\mathscr{V}|})}_{d[\omega_0 t]}(t)\right]^{\mathrm{T}},\\
\mathbf{I}^{(\mathscr{E})}_{q[\omega_0 t]}(t) &= \left[I^{(e_1)}_{q[\omega_0 t]}(t)\ I^{(e_2)}_{q[\omega_0 t]}(t)\ \cdots\ I^{(e_{|\mathscr{E}|})}_{q[\omega_0 t]}(t)\right]^{\mathrm{T}},\\
\mathbf{I}^{(\mathscr{E})}_{d[\omega_0 t]}(t) &= \left[I^{(e_1)}_{d[\omega_0 t]}(t)\ I^{(e_2)}_{d[\omega_0 t]}(t)\ \cdots\ I^{(e_{|\mathscr{E}|})}_{d[\omega_0 t]}(t)\right]^{\mathrm{T}}.
\end{aligned}$$

Then the network dynamics are described by:

$$\begin{aligned}
\frac{1}{\omega_0}\mathbf{L}^{(\mathscr{E})}\frac{d\mathbf{I}^{(\mathscr{E})}_{q[\omega_0 t]}(t)}{dt} &= -\mathbf{R}^{(\mathscr{E})}\mathbf{I}^{(\mathscr{E})}_{q[\omega_0 t]}(t) - \mathbf{L}^{(\mathscr{E})}\mathbf{I}^{(\mathscr{E})}_{d[\omega_0 t]}(t) + \mathbf{M}^{\mathrm{T}}\mathbf{V}^{(\mathscr{V})}_{q[\omega_0 t]}(t),\\
\frac{1}{\omega_0}\mathbf{L}^{(\mathscr{E})}\frac{d\mathbf{I}^{(\mathscr{E})}_{d[\omega_0 t]}(t)}{dt} &= -\mathbf{R}^{(\mathscr{E})}\mathbf{I}^{(\mathscr{E})}_{d[\omega_0 t]}(t) + \mathbf{L}^{(\mathscr{E})}\mathbf{I}^{(\mathscr{E})}_{q[\omega_0 t]}(t) + \mathbf{M}^{\mathrm{T}}\mathbf{V}^{(\mathscr{V})}_{d[\omega_0 t]}(t).
\end{aligned} \tag{11}$$

with

$$\begin{aligned}
\mathbf{R}^{(\mathscr{E})} &= \operatorname{diag}\left(R^{(e_1)}, R^{(e_2)}, \cdots, R^{(e_{|\mathscr{E}|})}\right),\\
\mathbf{L}^{(\mathscr{E})} &= \operatorname{diag}\left(L^{(e_1)}, L^{(e_2)}, \cdots, L^{(e_{|\mathscr{E}|})}\right),
\end{aligned}$$

where $\operatorname{diag}\left(d^{(1)}, d^{(2)}, \cdots, d^{(n)}\right)$ is a diagonal matrix with diagonal entries $d^{(1)}, d^{(2)}, \ldots, d^{(n)}$; and $\mathbf{M}$ denotes the network incidence matrix as defined in Section 2.

3.3 Generic Element Model

Let $V^{(l_j)}_{q[\omega_0 t]}(t) - \mathrm{j}V^{(l_j)}_{d[\omega_0 t]}(t)$ denote the per-unit voltage at bus j, and let $I^{(l_j)}_{q[\omega_0 t]}(t) - \mathrm{j}I^{(l_j)}_{d[\omega_0 t]}(t)$ denote the per-unit current injection by an element (typically a load) at bus j. The dynamics can be described by a generic non-linear system of differential equations which we assume to be of the form:

$$\begin{aligned}
\mu_V^{(l_j)}\dot{V}_{q[\omega_0 t]}^{(l_j)}(t) &= q_V\left(V_{q[\omega_0 t]}^{(l_j)}(t), V_{d[\omega_0 t]}^{(l_j)}(t), I_{q[\omega_0 t]}^{(l_j)}(t), I_{d[\omega_0 t]}^{(l_j)}(t)\right),\\
\mu_V^{(l_j)}\dot{V}_{d[\omega_0 t]}^{(l_j)}(t) &= d_V\left(V_{q[\omega_0 t]}^{(l_j)}(t), V_{d[\omega_0 t]}^{(l_j)}(t), I_{q[\omega_0 t]}^{(l_j)}(t), I_{d[\omega_0 t]}^{(l_j)}(t)\right),\\
\mu_I^{(l_j)}\dot{I}_{q[\omega_0 t]}^{(l_j)}(t) &= q_I\left(V_{q[\omega_0 t]}^{(l_j)}(t), V_{d[\omega_0 t]}^{(l_j)}(t), I_{q[\omega_0 t]}^{(l_j)}(t), I_{d[\omega_0 t]}^{(l_j)}(t)\right),\\
\mu_I^{(l_j)}\dot{I}_{d[\omega_0 t]}^{(l_j)}(t) &= d_I\left(V_{q[\omega_0 t]}^{(l_j)}(t), V_{d[\omega_0 t]}^{(l_j)}(t), I_{q[\omega_0 t]}^{(l_j)}(t), I_{d[\omega_0 t]}^{(l_j)}(t)\right),
\end{aligned} \tag{12}$$

where $\mu_V^{(l_j)}$ and $\mu_I^{(l_j)}$ represent time constants of the generic element at bus j; and $q_V\left(\cdot,\cdot,\cdot,\cdot\right)$, $d_V\left(\cdot,\cdot,\cdot,\cdot\right)$, $q_I\left(\cdot,\cdot,\cdot,\cdot\right)$, and $d_I\left(\cdot,\cdot,\cdot,\cdot\right)$ are nonlinear functions of its state variables.

4 Microgrid Reduced-Order Model 1 (μROm1)

In this section, the singular perturbation techniques discussed in Section 2.3 are used to reduce the order (state-space dimension) of the μHOm to obtain μROm1.

Assumption 4.1 *For $\varepsilon_1 = 1\times 10^{-5}$, the dynamic properties of the μHOm are such that at each bus j:*

$$\begin{aligned}
\mathbf{x}_1(t) = \Bigg[&\delta^{(s_j)}(t)\ Q_f^{(s_j)}(t)\ P_f^{(s_j)}(t)\ I_{q[\omega_0 t]}^{(s_j)}(t)\ I_{d[\omega_0 t]}^{(s_j)}(t)\ \Phi_{q[\alpha^{(j)}(t)]}^{(s_j)}(t)\ \Phi_{d[\alpha^{(s_j)}(t)]}^{(j)}(t)\\
&\mathbf{I}_{q[\omega_0 t]}^{(\mathscr{E})}(t)\ \mathbf{I}_{d[\omega_0 t]}^{(\mathscr{E})}(t)\ I_{q[\omega_0 t]}^{(l_j)}(t)\ I_{d[\omega_0 t]}^{(l_j)}(t)\ V_{q[\omega_0 t]}^{(l_j)}(t)\ V_{d[\omega_0 t]}^{(l_j)}(t)\Bigg]^{\mathrm{T}},\\
\mathbf{z}_1(t) = \Bigg[&\Gamma_{q[\alpha^{(j)}(t)]}^{(s_j)}(t)\ \Gamma_{d[\alpha^{(j)}(t)]}^{(s_j)}(t)\ \Xi_{q[\alpha^{(j)}(t)]}^{(s_j)}(t)\ \Xi_{d[\alpha^{(j)}(t)]}^{(s_j)}(t)\ \hat{E}_{q[\omega_0 t]}^{(s_j)}(t)\ \hat{E}_{d[\omega_0 t]}^{(s_j)}(t)\Bigg]^{\mathrm{T}},
\end{aligned}$$

and $\mathbf{w}_1(t) = \left[E_{q[\omega_0 t]}^{(s_j)}(t)\ E_{d[\omega_0 t]}^{(s_j)}(t)\right]^{\mathrm{T}}$, the dynamics of $\mathbf{z}_1(t)$ are faster than those of $\mathbf{x}_1(t)$, and the μHOm can be expressed compactly as follows:

$$\begin{aligned}
\dot{\mathbf{x}}_1(t) &= f_1\left(\mathbf{x}_1(t), \mathbf{z}_1(t), \mathbf{w}_1(t), \varepsilon_1\right),\\
\varepsilon_1\dot{\mathbf{z}}_1(t) &= g_1\left(\mathbf{x}_1(t), \mathbf{z}_1(t), \mathbf{w}_1(t), \varepsilon_1\right),\\
\mathbf{0} &= h_1\left(\mathbf{x}_1(t), \mathbf{z}_1(t), \mathbf{w}_1(t), \varepsilon_1\right).
\end{aligned} \tag{13}$$

Assumption 4.2 *Equation 13 satisfies the conditions for Tikhonov's theorem, as presented in Section 2.3*

Given Assumptions 4.1–4.2, the μHOm can be reduced to the so-called Microgrid Reduced-Order Model 1 (μROm1).

The explicit ordinary differential equations (ODEs) that constitute μROm1 are as follows (see [9] pp. 25–28 for a detailed derivation of this result):

$$
\begin{aligned}
D_{\omega}^{(s_j)}\frac{d\delta^{(s_j)}(t)}{dt} &= P_r^{(s_j)} - P_f^{(s_j)}(t),\\
\frac{1}{\omega_c^{(s_j)}}\frac{dQ_f^{(s_j)}(t)}{dt} &= -Q_f^{(s_j)}(t) + E_{q[\omega_0 t]}^{(s_j)}(t) I_{d[\omega_0 t]}^{(s_j)}(t) - E_{d[\omega_0 t]}^{(s_j)}(t) I_{q[\omega_0 t]}^{(s_j)}(t),\\
\frac{1}{\omega_c^{(s_j)}}\frac{dP_f^{(s_j)}(t)}{dt} &= -P_f^{(s_j)}(t) + E_{q[\omega_0 t]}^{(s_j)}(t) I_{q[\omega_0 t]}^{(s_j)}(t) + E_{d[\omega_0 t]}^{(s_j)}(t) I_{d[\omega_0 t]}^{(s_j)}(t),\\
\mu_V^{(l_j)}\dot{V}_{q[\omega_0 t]}^{(l_j)}(t) &= q_V\left(V_{q[\omega_0 t]}^{(l_j)}(t), V_{d[\omega_0 t]}^{(l_j)}(t), I_{q[\omega_0 t]}^{(l_j)}(t), I_{d[\omega_0 t]}^{(l_j)}(t)\right),\\
\mu_V^{(l_j)}\dot{V}_{d[\omega_0 t]}^{(l_j)}(t) &= d_V\left(V_{q[\omega_0 t]}^{(l_j)}(t), V_{d[\omega_0 t]}^{(l_j)}(t), I_{q[\omega_0 t]}^{(l_j)}(t), I_{d[\omega_0 t]}^{(l_j)}(t)\right),\\
\mu_I^{(l_j)}\dot{I}_{q[\omega_0 t]}^{(l_j)}(t) &= q_I\left(V_{q[\omega_0 t]}^{(l_j)}(t), V_{d[\omega_0 t]}^{(l_j)}(t), I_{q[\omega_0 t]}^{(l_j)}(t), I_{d[\omega_0 t]}^{(l_j)}(t)\right),\\
\mu_I^{(l_j)}\dot{I}_{d[\omega_0 t]}^{(l_j)}(t) &= d_I\left(V_{q[\omega_0 t]}^{(l_j)}(t), V_{d[\omega_0 t]}^{(l_j)}(t), I_{q[\omega_0 t]}^{(l_j)}(t), I_{d[\omega_0 t]}^{(l_j)}(t)\right),\\
\frac{1}{\omega_0}\mathbf{L}^{(\mathscr{E})}\frac{d\mathbf{I}_{q[\omega_0 t]}^{(\mathscr{E})}(t)}{dt} &= -\mathbf{R}^{(\mathscr{E})}\mathbf{I}_{q[\omega_0 t]}^{(\mathscr{E})}(t) - \mathbf{L}^{(\mathscr{E})}\mathbf{I}_{d[\omega_0 t]}^{(\mathscr{E})}(t) + \mathbf{M}^{\mathrm{T}}\mathbf{V}_{q[\omega_0 t]}^{(\mathscr{V})}(t),\\
\frac{1}{\omega_0}\mathbf{L}^{(\mathscr{E})}\frac{d\mathbf{I}_{d[\omega_0 t]}^{(\mathscr{E})}(t)}{dt} &= -\mathbf{R}^{(\mathscr{E})}\mathbf{I}_{d[\omega_0 t]}^{(\mathscr{E})}(t) + \mathbf{L}^{(\mathscr{E})}\mathbf{I}_{q[\omega_0 t]}^{(\mathscr{E})}(t) + \mathbf{M}^{\mathrm{T}}\mathbf{V}_{d[\omega_0 t]}^{(\mathscr{V})}(t),\\
\frac{L^{(s_j)}}{\omega_0}\frac{dI_{q[\omega_0 t]}^{(s_j)}(t)}{dt} &= -R^{(s_j)}I_{q[\omega_0 t]}^{(s_j)}(t) - L^{(s_j)}I_{d[\omega_0 t]}^{(s_j)}(t) + E_{q[\omega_0 t]}^{(s_j)}(t) - V_{q[\omega_0 t]}^{(l_j)}(t),\\
\frac{L^{(s_j)}}{\omega_0}\frac{dI_{d[\omega_0 t]}^{(s_j)}(t)}{dt} &= L^{(s_j)}I_{q[\omega_0 t]}^{(s_j)}(t) - R^{(s_j)}I_{d[\omega_0 t]}^{(s_j)}(t) + E_{d[\omega_0 t]}^{(s_j)}(t) - V_{d[\omega_0 t]}^{(l_j)}(t),\\
\frac{1}{\omega_0}\frac{d\Phi_{q[\alpha^{(j)}(t)]}^{(s_j)}(t)}{dt} &= -\frac{K_{I\phi}^{(s_j)}K_{P\phi}^{(s_j)}}{C^{(s_j)2}\left(1+K_{P\phi}^{(s_j)}\hat{R}_0^{(s_j)}\right)^2 + \left(K_{P\phi}^{(s_j)}\right)^2}\Phi_{q[\alpha^{(j)}(t)]}^{(s_j)}(t)\\
&\quad + \frac{C^{(s_j)}K_{I\phi}^{(s_j)}}{C^{(s_j)2}\left(1+K_{P\phi}^{(s_j)}\hat{R}_0^{(s_j)}\right)^2 + \left(K_{P\phi}^{(s_j)}\right)^2}\Phi_{d[\alpha^{(j)}(t)]}^{(s_j)}(t)\\
&\quad + \frac{K_{P\phi}^{(s_j)}\left(I_{q[\omega_0 t]}^{(s_j)}(t)\cos(\delta^{(s_j)}(t)) - I_{d[\omega_0 t]}^{(s_j)}(t)\sin(\delta^{(s_j)}(t))\right)}{C^{(s_j)2}\left(1+K_{P\phi}^{(s_j)}\hat{R}_0^{(s_j)}\right)^2 + \left(K_{P\phi}^{(s_j)}\right)^2}\\
&\quad + \frac{C^{(s_j)2}\left(1+K_{P\phi}^{(s_j)}\hat{R}_0^{(s_j)}\right)^2 E_0^{(s_j)}}{C^{(s_j)2}\left(1+K_{P\phi}^{(s_j)}\hat{R}_0^{(s_j)}\right)^2 + \left(K_{P\phi}^{(s_j)}\right)^2}\\
&\quad + \frac{C^{(s_j)2}\left(1+K_{P\phi}^{(s_j)}\hat{R}_0^{(s_j)}\right)^2\left(Q_r^{(s_j)} - Q_f^{(s_j)}(t)\right)}{D_E^{(s_j)}C^{(s_j)2}\left(1+K_{P\phi}^{(s_j)}\hat{R}_0^{(s_j)}\right)^2 + D_E^{(s_j)}\left(K_{P\phi}^{(s_j)}\right)^2},
\end{aligned}
$$

$$\begin{aligned}\frac{1}{\omega_0}\frac{d\Phi^{(s_j)}_{d[\alpha^{(j)}(t)]}(t)}{dt} =& -\frac{K^{(s_j)}_{I\phi}K^{(s_j)}_{P\phi}}{C^{(s_j)^2}\left(1+K^{(s_j)}_{P\phi}\hat{R}^{(s_j)}_0\right)^2+\left(K^{(s_j)}_{P\phi}\right)^2}\Phi^{(s_j)}_{d[\alpha^{(j)}(t)]}(t)\\ &+\frac{C^{(s_j)}K^{(s_j)}_{I\phi}}{C^{(s_j)^2}\left(1+K^{(s_j)}_{P\phi}\hat{R}^{(s_j)}_0\right)^2+\left(K^{(s_j)}_{P\phi}\right)^2}\Phi^{(s_j)}_{q[\alpha^{(j)}(t)]}(t)\\ &+\frac{K^{(s_j)}_{P\phi}\left(I^{(s_j)}_{q[\omega_0 t]}(t)\sin(\delta^{(s_j)}(t))+I^{(s_j)}_{d[\omega_0 t]}(t)cos(\delta^{(s_j)}(t))\right)}{C^{(s_j)^2}\left(1+K^{(s_j)}_{P\phi}\hat{R}^{(s_j)}_0\right)^2+\left(K^{(s_j)}_{P\phi}\right)^2}\\ &-\frac{C^{(s_j)}K^{(s_j)}_{P\phi}\left(E^{(s_j)}_0+\frac{1}{D^{(s_j)}_E}\left(Q^{(s_j)}_r-Q^{(s_j)}_f(t)\right)\right)}{C^{(s_j)^2}\left(1+K^{(s_j)}_{P\phi}\hat{R}^{(s_j)}_0\right)^2+\left(K^{(s_j)}_{P\phi}\right)^2},\end{aligned}$$

where

$$\begin{aligned}E^{(s_j)}_{q[\omega_0 t]}(t) =& -\frac{K^{(s_j)}_{P\phi}}{C^{(s_j)^2}\left(1+K^{(s_j)}_{P\phi}\hat{R}^{(s_j)}_0\right)^2+\left(K^{(s_j)}_{P\phi}\right)^2}I^{(s_j)}_{q[\omega_0 t]}(t)\\ &+\frac{C^{(s_j)}K^{(s_j)}_{I\phi}\left(\Phi^{(s_j)}_{q[\alpha^{(j)}(t)]}(t)\sin(\delta^{(s_j)}(t))-\Phi^{(s_j)}_{d[\alpha^{(j)}(t)]}(t)\cos(\delta^{(s_j)}(t))\right)}{C^{(s_j)^2}\left(1+K^{(s_j)}_{P\phi}\hat{R}^{(s_j)}_0\right)^2+\left(K^{(s_j)}_{P\phi}\right)^2}\\ &+\frac{K^{(s_j)}_{I\phi}K^{(s_j)}_{P\phi}\left(\Phi^{(s_j)}_{q[\alpha^{(j)}(t)]}(t)\cos(\delta^{(s_j)}(t))+\Phi^{(s_j)}_{d[\alpha^{(j)}(t)]}(t)\sin(\delta^{(s_j)}(t))\right)}{C^{(s_j)^2}\left(1+K^{(s_j)}_{P\phi}\hat{R}^{(s_j)}_0\right)^2+\left(K^{(s_j)}_{P\phi}\right)^2}\\ &+\frac{E^{(s_j)}_0C^{(s_j)}K^{(s_j)}_{P\phi}\left(1+K^{(s_j)}_{P\phi}\hat{R}^{(s_j)}_0\right)\sin(\delta^{(s_j)}(t))}{C^{(s_j)^2}\left(1+K^{(s_j)}_{P\phi}\hat{R}^{(s_j)}_0\right)^2+\left(K^{(s_j)}_{P\phi}\right)^2}\\ &+\frac{C^{(s_j)}K^{(s_j)}_{P\phi}\left(1+K^{(s_j)}_{P\phi}\hat{R}^{(s_j)}_0\right)\left(Q^{(s_j)}_r-Q^{(s_j)}_f(t)\right)\sin(\delta^{(s_j)}(t))}{D^{(s_j)}_EC^{(s_j)^2}\left(1+K^{(s_j)}_{P\phi}\hat{R}^{(s_j)}_0\right)^2+D^{(s_j)}_E\left(K^{(s_j)}_{P\phi}\right)^2}\\ &+\frac{\left(K^{(s_j)}_{P\phi}\right)^2\cos(\delta^{(s_j)}(t))\left(E^{(s_j)}_0+\frac{1}{D^{(s_j)}_E}\left(Q^{(s_j)}_r-Q^{(s_j)}_f(t)\right)\right)}{C^{(s_j)^2}\left(1+K^{(s_j)}_{P\phi}\hat{R}^{(s_j)}_0\right)^2+\left(K^{(s_j)}_{P\phi}\right)^2},\end{aligned}$$

$$
\begin{aligned}
E^{(s_j)}_{d[\omega_0 t]}(t) = &- \frac{K^{(s_j)}_{P\phi}}{{C^{(s_j)}}^2\left(1+K^{(s_j)}_{P\phi}\hat{R}^{(s_j)}_0\right)^2+\left(K^{(s_j)}_{P\phi}\right)^2} I^{(s_j)}_{d[\omega_0 t]}(t) \\
&+ \frac{C^{(s_j)}K^{(s_j)}_{I\phi}\left(\Phi^{(s_j)}_{q[\alpha^{(j)}(t)]}(t)\cos(\delta^{(s_j)}(t))+\Phi^{(s_j)}_{d[\alpha^{(j)}(t)]}(t)\sin(\delta^{(s_j)}(t))\right)}{{C^{(s_j)}}^2\left(1+K^{(s_j)}_{P\phi}\hat{R}^{(s_j)}_0\right)^2+\left(K^{(s_j)}_{P\phi}\right)^2} \\
&- \frac{K^{(s_j)}_{I\phi}K^{(s_j)}_{P\phi}\left(\Phi^{(s_j)}_{q[\alpha^{(j)}(t)]}(t)\sin(\delta^{(s_j)}(t))-\Phi^{(s_j)}_{d[\alpha^{(j)}(t)]}(t)\cos(\delta^{(s_j)}(t))\right)}{{C^{(s_j)}}^2\left(1+K^{(s_j)}_{P\phi}\hat{R}^{(s_j)}_0\right)^2+\left(K^{(s_j)}_{P\phi}\right)^2} \\
&+ \frac{E^{(s_j)}_0 C^{(s_j)}K^{(s_j)}_{P\phi}\left(1+K^{(s_j)}_{P\phi}\hat{R}^{(s_j)}_0\right)\cos(\delta^{(s_j)}(t))}{{C^{(s_j)}}^2\left(1+K^{(s_j)}_{P\phi}\hat{R}^{(s_j)}_0\right)^2+\left(K^{(s_j)}_{P\phi}\right)^2} \\
&+ \frac{C^{(s_j)}K^{(s_j)}_{P\phi}\left(1+K^{(s_j)}_{P\phi}\hat{R}^{(s_j)}_0\right)\left(Q^{(s_j)}_r-Q^{(s_j)}_f(t)\right)\cos(\delta^{(s_j)}(t))}{D^{(s_j)}_E{C^{(s_j)}}^2\left(1+K^{(s_j)}_{P\phi}\hat{R}^{(s_j)}_0\right)^2+D^{(s_j)}_E\left(K^{(s_j)}_{P\phi}\right)^2} \\
&- \frac{\left(K^{(s_j)}_{P\phi}\right)^2\sin(\delta^{(s_j)}(t))\left(E^{(s_j)}_0+\frac{1}{D^{(s_j)}_E}\left(Q^{(s_j)}_r-Q^{(s_j)}_f(t)\right)\right)}{{C^{(s_j)}}^2\left(1+K^{(s_j)}_{P\phi}\hat{R}^{(s_j)}_0\right)^2+\left(K^{(s_j)}_{P\phi}\right)^2}.
\end{aligned}
$$

5 Microgrid Reduced-Order Model 2 (μROm2)

In this section, the singular perturbation techniques discussed in Section 2.3 are used to reduce the order (state-space dimension) of the μHOm to obtain μROm2.

Assumption 5.1 *For $\varepsilon_2 = 1\times 10^{-3}$, the dynamic properties of the μHOm are such that at each bus j:*

$$
\begin{aligned}
\mathbf{z}_2(t) = \Big[&I^{(l_j)}_{q[\omega_0 t]}(t)\ I^{(l_j)}_{d[\omega_0 t]}(t)\ V^{(l_j)}_{q[\omega_0 t]}(t)\ V^{(l_j)}_{d[\omega_0 t]}(t)\ \mathbf{I}^{(\mathscr{E})}_{q[\omega_0 t]}(t)\ \mathbf{I}^{(\mathscr{E})}_{d[\omega_0 t]}(t)\ I^{(s_j)}_{q[\omega_0 t]}(t)\ I^{(s_j)}_{d[\omega_0 t]}(t) \\
&\Phi^{(s_j)}_{q[\alpha^{(j)}(t)]}(t)\ \Phi^{(s_j)}_{d[\alpha^{(j)}(t)]}(t)\ \Gamma^{(s_j)}_{q[\alpha^{(j)}(t)]}(t)\ \Gamma^{(s_j)}_{d[\alpha^{(j)}(t)]}(t)\ \Xi^{(s_j)}_{q[\alpha^{(j)}(t)]}(t)\ \Xi^{(s_j)}_{d[\alpha^{(j)}(t)]}(t) \\
&\hat{E}^{(s_j)}_{q[\omega_0 t]}(t)\ \hat{E}^{(s_j)}_{d[\omega_0 t]}(t)\Big]^{\mathrm{T}},
\end{aligned}
$$

$\mathbf{x}_2(t) = \left[\delta^{(s_j)}(t)\ Q^{(s_j)}_f(t)\ P^{(s_j)}_f(t)\right]^{\mathrm{T}}$, *and* $\mathbf{w}_2(t) = \left[E^{(s_j)}_{q[\omega_0 t]}(t)\ E^{(s_j)}_{d[\omega_0 t]}(t)\right]^{\mathrm{T}}$, *the dynamics of $\mathbf{z}_2(t)$ are faster than those of $\mathbf{x}_2(t)$, and the μHOm can be expressed compactly as follows:*

$$\begin{aligned}\dot{\mathbf{x}}_2(t) &= f_2\left(\mathbf{x}_2(t),\mathbf{z}_2(t),\mathbf{w}_2(t),\varepsilon_2\right),\\ \varepsilon_2\dot{\mathbf{z}}_2(t) &= g_2\left(\mathbf{x}_2(t),\mathbf{z}_2(t),\mathbf{w}_2(t),\varepsilon_2\right),\\ \mathbf{0} &= h_2\left(\mathbf{x}_2(t),\mathbf{z}_2(t),\mathbf{w}_2(t),\varepsilon_2\right).\end{aligned} \tag{14}$$

Assumption 5.2 *Equation 14 satisfies the conditions for Tikhonov's theorem, as presented in Section 2.3*

Given Assumptions 5.1–5.2, the μHOm can be reduced to the so-called Microgrid Reduced-Order Model 2 (μROm2) using the developments in Section 2.3.

Let $\theta^{(s_j)}(t) \coloneqq \arctan\left(\frac{-E^{(s_j)}_{d[\omega_0 t]}(t)}{E^{(s_j)}_{q[\omega_0 t]}(t)}\right)$, and $\theta^{(l_j)}(t) \coloneqq \arctan\left(\frac{-V^{(l_j)}_{d[\omega_0 t]}(t)}{V^{(l_j)}_{q[\omega_0 t]}(t)}\right)$. Let $\beta^{(j)} \in \{0,1\}$ be a constant such that $\beta^{(j)} = 1$ if bus $j \in \mathscr{V}_{\mathscr{G}}$, and $\beta^{(j)} = 0$ otherwise. Also, let $\left|\overrightarrow{\mathbf{V}}^{(e_m)}(t)\right| = \left|\overrightarrow{\mathbf{V}}^{(l_j)}(t)\right|\left|\overrightarrow{\mathbf{V}}^{(l_k)}(t)\right|$, and

$$\begin{aligned}&\text{at bus } j: \quad \theta^{(e_m)}(t) = \theta^{(l_j)}(t) - \theta^{(l_k)}(t),\\ &\text{at bus } k: \quad \theta^{(e_m)}(t) = \theta^{(l_k)}(t) - \theta^{(l_j)}(t).\end{aligned}$$

Assumption 5.3 *The generic model in* (12) *can be reduced to the so called ZIP model (see e.g. [12]), given by:*

$$\begin{aligned}V^{(l_j)}_{q[\omega_0 t]}(t)I^{(l_j)}_{q[\omega_0 t]}(t) + V^{(l_j)}_{d[\omega_0 t]}(t)I^{(l_j)}_{d[\omega_0 t]}(t) &= -P^{(l_j)}_0 - \left|\overrightarrow{\mathbf{V}}^{(l_j)}(t)\right| P^{(l_j)}_1 - \left|\overrightarrow{\mathbf{V}}^{(l_j)}(t)\right|^2 P^{(l_j)}_2,\\ V^{(l_j)}_{q[\omega_0 t]}(t)I^{(l_j)}_{d[\omega_0 t]}(t) - V^{(l_j)}_{d[\omega_0 t]}(t)I^{(l_j)}_{q[\omega_0 t]}(t) &= -Q^{(l_j)}_0 - \left|\overrightarrow{\mathbf{V}}^{(l_j)}(t)\right| Q^{(l_j)}_1 - \left|\overrightarrow{\mathbf{V}}^{(l_j)}(t)\right|^2 Q^{(l_j)}_2,\end{aligned}$$

where $P^{(l_j)}_0$, $P^{(l_j)}_1$, $P^{(l_j)}_2$, $Q^{(l_j)}_0$, $Q^{(l_j)}_1$ and $Q^{(l_j)}_2$ denote constants for the element at bus j, and $\left|\overrightarrow{\mathbf{V}}^{(l_j)}(t)\right|$ denotes the phasor magnitude of $V^{(l_j)}_{q[\omega_0 t]}(t) - \mathrm{j}V^{(l_j)}_{d[\omega_0 t]}(t)$.

The explicit ordinary differential equations (ODEs) that constitute μROm2 are as follows (see [9] pp. 31–36 for a detailed derivation of this result):

$$D_{\omega}^{(s_j)}\frac{d\theta^{(s_j)}(t)}{dt} = P_r^{(s_j)} - P_f^{(s_j)}(t),$$

$$\frac{1}{\omega_c^{(s_j)}}\frac{dQ_f^{(s_j)}(t)}{dt} = -B^{(s_j)}\left|\overrightarrow{\mathbf{V}}^{(l_j)}(t)\right|^2 - \left|\overrightarrow{\mathbf{V}}^{(l_j)}(t)\right|\left|\overrightarrow{\mathbf{E}}^{(s_j)}(t)\right|\left(G^{(s_j)}\sin\left(\theta^{(s_j)}(t) - \theta^{(l_j)}(t)\right) - B^{(s_j)}\cos\left(\theta^{(s_j)}(t) - \theta^{(l_j)}(t)\right)\right) - Q_f^{(s_j)}(t),$$

$$\frac{1}{\omega_c^{(s_j)}}\frac{dP_f^{(s_j)}(t)}{dt} = G^{(s_j)}\left|\overrightarrow{\mathbf{E}}^{(s_j)}(t)\right|^2 - \left|\overrightarrow{\mathbf{V}}^{(l_j)}(t)\right|\left|\overrightarrow{\mathbf{E}}^{(s_j)}(t)\right|\left(G^{(s_j)}\cos\left(\theta^{(s_j)}(t) - \theta^{(l_j)}(t)\right) + B^{(s_j)}\sin\left(\theta^{(s_j)}(t) - \theta^{(l_j)}(t)\right)\right) - P_f^{(s_j)}(t),$$

and for $E(j)$ representing the set of edges incident to node j, such that $e_m \in E(j)$ if and only if the edge e_m is incident to node j, the power balance equations at bus $j \in \mathscr{V}$ are given by:

$$\begin{aligned}
0 = {} & P_0^{(l_j)} + \left|\overrightarrow{\mathbf{V}}^{(l_j)}(t)\right| P_1^{(l_j)} + \left|\overrightarrow{\mathbf{V}}^{(l_j)}(t)\right|^2 P_2^{(l_j)} + \beta^{(j)} G^{(s_j)}\left|V^{(l_j)}(t)\right|^2 \\
& - \beta^{(j)}\left|\overrightarrow{\mathbf{V}}^{(l_j)}(t)\right|\left|\overrightarrow{\mathbf{E}}^{(s_j)}(t)\right|\left(G^{(s_j)}\cos\left(\theta^{(l_j)}(t) - \theta^{(s_j)}(t)\right)\right. \\
& \left. + B^{(s_j)}\sin\left(\theta^{(l_j)}(t) - \theta^{(s_j)}(t)\right)\right) + \left|\overrightarrow{\mathbf{V}}^{(l_j)}(t)\right|^2 \sum_{e_m \in E(j)} G^{(e_m)} \\
& - \sum_{e_m \in E(j)}\left|\overrightarrow{\mathbf{V}}^{(e_m)}(t)\right|\left(G^{(e_m)}\cos\left(\theta^{(e_m)}(t)\right) + B^{(e_m)}\sin\left(\theta^{(e_m)}(t)\right)\right), \\
0 = {} & Q_0^{(l_j)} + \left|\overrightarrow{\mathbf{V}}^{(l_j)}(t)\right| Q_1^{(l_j)} + \left|\overrightarrow{\mathbf{V}}^{(l_j)}(t)\right|^2 Q_2^{(l_j)} - \beta^{(j)} B^{(l_j)}\left|\overrightarrow{\mathbf{V}}^{(l_j)}(t)\right|^2 \\
& - \beta^{(j)}\left|\overrightarrow{\mathbf{V}}^{(l_j)}(t)\right|\left|\overrightarrow{\mathbf{E}}^{(s_j)}(t)\right|\left(G^{(s_j)}\sin\left(\theta^{(l_j)}(t) - \theta^{(s_j)}(t)\right)\right. \\
& \left. - B^{(s_j)}\cos\left(\theta^{(l_j)}(t) - \theta^{(s_j)}(t)\right)\right) - \left|\overrightarrow{\mathbf{V}}^{(l_j)}(t)\right|^2 \sum_{e_m \in E(j)} B^{(e_m)} \\
& - \sum_{e_m \in E(j)}\left|\overrightarrow{\mathbf{V}}^{(e_m)}(t)\right|\left(G^{(e_m)}\sin\left(\theta^{(e_m)}(t)\right) - B^{(e_m)}\cos\left(\theta^{(e_m)}(t)\right)\right).
\end{aligned}$$

and

$$\left|\overrightarrow{\mathbf{E}}^{(s_j)}(t)\right| = \frac{\left(K_{P\phi}^{(s_j)}\right)^2\left(E_0^{(s_j)} + \frac{1}{D_E^{(s_j)}}\left(Q_r^{(s_j)} - Q_f^{(s_j)}(t)\right)\right)}{C^{(s_j)2}\left(1 + K_{P\phi}^{(s_j)}\hat{R}_0^{(s_j)}\right)^2 + \left(K_{P\phi}^{(s_j)}\right)^2}.$$

where $\hat{G}^{(s_j)} = \frac{\hat{R}_0^{(s_j)}}{\left(\hat{R}_0^{(s_j)}\right)^2+\left(\frac{1}{C^{(s_j)}}\right)^2}$, $\hat{B}^{(s_j)} = \frac{C^{(s_j)}}{\left(C^{(s_j)}\hat{R}_0^{(s_j)}\right)^2+1}$, $G^{(s_j)} = \frac{R^{(s_j)}}{\left(R^{(s_j)}\right)^2+\left(L^{(s_j)}\right)^2}$, $B^{(s_j)} = \frac{-L^{(s_j)}}{\left(R^{(s_j)}\right)^2+\left(L^{(s_j)}\right)^2}$, $G^{(e_m)} = \frac{R^{(e_m)}}{\left(R^{(e_m)}\right)^2+\left(L^{(e_m)}\right)^2}$, and $B^{(e_m)} = \frac{-L^{(e_m)}}{\left(R^{(e_m)}\right)^2+\left(L^{(e_m)}\right)^2}$.

6 Microgrid Reduced-Order Model 3 (μROm3)

In this section, the singular perturbation techniques discussed in Section 2.3 are used to reduce the order (state-space dimension) of the μHOm to obtain μROm3.

Assumption 6.1 *For $\varepsilon_3 = 1\times10^{-1}$, the dynamic properties of the μHOm are such that at each bus j:*

$$\mathbf{z}_3(t) = \Big[Q_f^{(s_j)}(t)\ P_f^{(s_j)}(t)\ I_{q[\omega_0 t]}^{(l_j)}(t)\ I_{d[\omega_0 t]}^{(l_j)}(t)\ V_{q[\omega_0 t]}^{(l_j)}(t)\ V_{d[\omega_0 t]}^{(l_j)}(t)\ \mathbf{I}_{q[\omega_0 t]}^{(\mathscr{E})}(t)\ \mathbf{I}_{d[\omega_0 t]}^{(\mathscr{E})}(t)\ I_{q[\omega_0 t]}^{(s_j)}(t)\ I_{d[\omega_0 t]}^{(s_j)}(t)\ \Phi_{q[\alpha^{(j)}(t)]}^{(s_j)}(t)\ \Phi_{d[\alpha^{(j)}(t)]}^{(s_j)}(t)\ \Gamma_{q[\alpha^{(j)}(t)]}^{(s_j)}(t)\ \Gamma_{d[\alpha^{(j)}(t)]}^{(s_j)}(t)\ \Xi_{q[\alpha^{(j)}(t)]}^{(s_j)}(t)\ \Xi_{d[\alpha^{(j)}(t)]}^{(s_j)}(t)\ \hat{E}_{q[\omega_0 t]}^{(s_j)}(t)\ \hat{E}_{d[\omega_0 t]}^{(s_j)}(t)\Big]^{\mathrm{T}},$$

$\mathbf{x}_3(t) = \delta^{(s_j)}(t)$, *and* $\mathbf{w}_3(t) = \left[E_{q[\omega_0 t]}^{(s_j)}(t)\ E_{d[\omega_0 t]}^{(s_j)}(t)\right]^{\mathrm{T}}$, *the dynamics of $\mathbf{z}_3(t)$ are faster than those of $\mathbf{x}_3(t)$, and the μHOm can be expressed compactly as follows:*

$$\begin{aligned}\dot{\mathbf{x}}_3(t) &= f_3\left(\mathbf{x}_3(t),\mathbf{z}_3(t),\mathbf{w}_3(t),\varepsilon_3\right),\\ \varepsilon_3\dot{\mathbf{z}}_3(t) &= g_3\left(\mathbf{x}_3(t),\mathbf{z}_3(t),\mathbf{w}_3(t),\varepsilon_3\right),\\ \mathbf{0} &= h_3\left(\mathbf{x}_3(t),\mathbf{z}_3(t),\mathbf{w}_3(t),\varepsilon_3\right).\end{aligned} \tag{15}$$

Assumption 6.2 *Equation 15 satisfies the conditions for Tikhonov's theorem, as presented in Section 2.3*

Given Assumptions 6.1–6.2, the μHOm can be reduced to the so-called Microgrid Reduced-Order Model 3 (μROm3).

Using Assumption 5.3 and the definitions in Section 5, the explicit ordinary differential equations (ODEs) that constitute μROm3 are as follows (see [9] pp. 37–41 for a detailed derivation of this result):

$$D_\omega^{(s_j)}\frac{d\theta^{(s_j)}(t)}{dt} = P_r^{(s_j)} - G^{(s_j)}\left|\overrightarrow{\mathbf{E}}^{(s_j)}(t)\right|^2 + \left|\overrightarrow{\mathbf{V}}^{(l_j)}(t)\right|\left|\overrightarrow{\mathbf{E}}^{(s_j)}(t)\right|\Big(G^{(s_j)}\cos\Big(\theta^{(s_j)}(t) - \theta^{(l_j)}(t)\Big) + B^{(s_j)}\sin\Big(\theta^{(s_j)}(t) - \theta^{(l_j)}(t)\Big)\Big),$$

$$\left|\overrightarrow{\mathbf{E}}^{(s_j)}(t)\right| = \frac{1}{D_E^{(s_j)}}\Bigg(Q_r^{(s_j)} + B^{(s_j)}\left|\overrightarrow{\mathbf{V}}^{(l_j)}(t)\right|^2 + \left|\overrightarrow{\mathbf{V}}^{(l_j)}(t)\right|\left|\overrightarrow{\mathbf{E}}^{(s_j)}(t)\right|\Big(G^{(s_j)}\sin\Big(\theta^{(s_j)}(t) - \theta^{(l_j)}(t)\Big) - B^{(s_j)}\cos\Big(\theta^{(s_j)}(t) - \theta^{(l_j)}(t)\Big)\Big)\Bigg) + E_0^{(s_j)},$$

and for $E(j)$ representing the set of edges incident to node j, such that $e_m \in E(j)$ if and only if the edge e_m is incident to node j, the power balance equations at bus $j \in \mathscr{V}$ are given by:

$$\begin{aligned}
0 = {} & P_0^{(l_j)} + \left|\overrightarrow{\mathbf{V}}^{(l_j)}(t)\right|P_1^{(l_j)} + \left|\overrightarrow{\mathbf{V}}^{(l_j)}(t)\right|^2 P_2^{(l_j)} + \beta^{(j)}G^{(s_j)}\left|V^{(l_j)}(t)\right|^2 \\
& - \beta^{(j)}\left|\overrightarrow{\mathbf{V}}^{(l_j)}(t)\right|\left|\overrightarrow{\mathbf{E}}^{(s_j)}(t)\right|\Big(G^{(s_j)}\cos\Big(\theta^{(l_j)}(t) - \theta^{(s_j)}(t)\Big) \\
& + B^{(s_j)}\sin\Big(\theta^{(l_j)}(t) - \theta^{(s_j)}(t)\Big)\Big) + \left|\overrightarrow{\mathbf{V}}^{(l_j)}(t)\right|^2 \sum_{e_m \in E(j)} G^{(e_m)} \\
& - \sum_{e_m \in E(j)}\left|\overrightarrow{\mathbf{V}}^{(e_m)}(t)\right|\Big(G^{(e_m)}\cos\Big(\theta^{(e_m)}(t)\Big) + B^{(e_m)}\sin\Big(\theta^{(e_m)}(t)\Big)\Big), \\
0 = {} & Q_0^{(l_j)} + \left|\overrightarrow{\mathbf{V}}^{(l_j)}(t)\right|Q_1^{(l_j)} + \left|\overrightarrow{\mathbf{V}}^{(l_j)}(t)\right|^2 Q_2^{(l_j)} - \beta^{(j)}B^{(l_j)}\left|\overrightarrow{\mathbf{V}}^{(l_j)}(t)\right|^2 \\
& - \beta^{(j)}\left|\overrightarrow{\mathbf{V}}^{(l_j)}(t)\right|\left|\overrightarrow{\mathbf{E}}^{(s_j)}(t)\right|\Big(G^{(s_j)}\sin\Big(\theta^{(l_j)}(t) - \theta^{(s_j)}(t)\Big) \\
& - B^{(s_j)}\cos\Big(\theta^{(l_j)}(t) - \theta^{(s_j)}(t)\Big)\Big) - \left|\overrightarrow{\mathbf{V}}^{(l_j)}(t)\right|^2 \sum_{e_m \in E(j)} B^{(e_m)} \\
& - \sum_{e_m \in E(j)}\left|\overrightarrow{\mathbf{V}}^{(e_m)}(t)\right|\Big(G^{(e_m)}\sin\Big(\theta^{(e_m)}(t)\Big) - B^{(e_m)}\cos\Big(\theta^{(e_m)}(t)\Big)\Big).
\end{aligned}$$

where $\hat{G}^{(s_j)} = \frac{\hat{R}_0^{(s_j)}}{\left(\hat{R}_0^{(s_j)}\right)^2 + \left(\frac{1}{C^{(s_j)}}\right)^2}$, $\hat{B}^{(s_j)} = \frac{C^{(s_j)}}{\left(C^{(s_j)}\hat{R}_0^{(s_j)}\right)^2 + 1}$, $G^{(s_j)} = \frac{R^{(s_j)}}{\left(R^{(s_j)}\right)^2 + \left(L^{(s_j)}\right)^2}$, $B^{(s_j)} = \frac{-L^{(s_j)}}{\left(R^{(s_j)}\right)^2 + \left(L^{(s_j)}\right)^2}$, $G^{(e_m)} = \frac{R^{(e_m)}}{\left(R^{(e_m)}\right)^2 + \left(L^{(e_m)}\right)^2}$, and $B^{(e_m)} = \frac{-L^{(e_m)}}{\left(R^{(e_m)}\right)^2 + \left(L^{(e_m)}\right)^2}$.

7 Comparison of μHOm and μROm

In this section, the time resolution for the reduced-order models is discussed, and for given test cases, the responses of μHOm, μROm1, μROm2 and μROm3 are compared and validated.

7.1 Reduced-Model Time Resolution

For formulation of μROmi $i = 1,2,3$, the value for ε_i was chosen such that $\frac{1}{10\varepsilon_i}$ represents the largest eigenvalues of the system, associated with the fast states $\mathbf{z}_i(t)$. Consequently, the fast-varying terms in the system response reach steady state in approximately $50\varepsilon_i$ seconds, and the time resolution of μROmi is $50\varepsilon_i$ seconds. Table 1 shows the time resolution for the reduced-order models.

Table 1: Reduced-Model Time Resolution

	small parameter	*time-scale*
μROm1	$\varepsilon_1 = 1\times10^{-5}$	500 μs
μROm2	$\varepsilon_2 = 1\times10^{-3}$	50 ms
μROm3	$\varepsilon_3 = 0.1$	5 s

7.2 Model Validation

To validate the μHOm, μROm1, μROm2 and μROm3, the following test case is employed: two grid-forming inverters based battery sources connected to a 3-bus microgrid electrical network with an *RLC* load. One inverter-interfaced source is connected to bus 1 and the other to bus 2, and the load is connected to bus 3. Using the μHOm, μROm1, μROm2 and μROm3, we developed the test case in Simulink. The model parameters are shown in Table 2.

Let $I^{(l_3)}_{q[\omega_0 t]}(t) - \mathrm{j}I^{(l_3)}_{d[\omega_0 t]}(t)$ denote the current across the load inductance. The load model used in μHOm and μROm1 is given by:

$$\frac{C^{(l_3)}}{\omega_0}\frac{dV^{(l_3)}_{q[\omega_0 t]}(t)}{dt} = -\frac{1}{R^{(l_3)}}V^{(l_3)}_{q[\omega_0 t]}(t) - C^{(l_3)}V^{(l_3)}_{d[\omega_0 t]}(t) - I^{(l_3)}_{lq[\omega_0 t]}(t) + I^{(l_3)}_{q[\omega_0 t]}(t), \quad (16)$$

$$\frac{C^{(l_3)}}{\omega_0}\frac{dV^{(l_3)}_{d[\omega_0 t]}(t)}{dt} = -\frac{1}{R^{(l_3)}}V^{(l_3)}_{d[\omega_0 t]}(t) + C^{(l_3)}V^{(l_3)}_{q[\omega_0 t]}(t) - I^{(l_3)}_{ld[\omega_0 t]}(t) + I^{(l_3)}_{d[\omega_0 t]}(t), \quad (17)$$

$$\frac{L^{(l_3)}}{\omega_0}\frac{dI^{(l_3)}_{lq[\omega_0 t]}(t)}{dt} = -L^{(l_3)}I^{(l_3)}_{ld[\omega_0 t]}(t) + V^{(l_3)}_{q[\omega_0 t]}(t), \tag{18}$$

$$\frac{L^{(l_3)}}{\omega_0}\frac{dI^{(l_3)}_{ld[\omega_0 t]}(t)}{dt} = L^{(l_3)}I^{(l_3)}_{lq[\omega_0 t]}(t) + V^{(l_3)}_{d[\omega_0 t]}(t), \tag{19}$$

The load model used in μROm2 and μROm3 is given by:

$$\begin{aligned} V^{(l_3)}_{q[\omega_0 t]}(t) = {} & \frac{R^{(l_3)}}{1+\left(R^{(l_3)}C^{(l_3)}\right)^2}\left(I^{(l_3)}_{q[\omega_0 t]}(t) + \frac{V^{(l_3)}_{d[\omega_0 t]}(t)}{L^{(l_3)}}\right) \\ & - \frac{\left(R^{(l_3)}\right)^2 C^{(l_3)}}{1+\left(R^{(l_3)}C^{(l_3)}\right)^2}\left(I^{(l_3)}_{d[\omega_0 t]}(t) - \frac{V^{(l_3)}_{q[\omega_0 t]}(t)}{L^{(l_3)}}\right), \end{aligned} \tag{20}$$

$$\begin{aligned} V^{(l_3)}_{d[\omega_0 t]}(t) = {} & \frac{\left(R^{(l_3)}\right)^2 C^{(l_3)}}{1+\left(R^{(l_3)}C^{(l_3)}\right)^2}\left(I^{(l_3)}_{q[\omega_0 t]}(t) + \frac{V^{(l_3)}_{d[\omega_0 t]}(t)}{L^{(l_3)}}\right) \\ & + \frac{R^{(l_3)}}{1+\left(R^{(l_3)}C^{(l_3)}\right)^2}\left(I^{(l_3)}_{d[\omega_0 t]}(t) - \frac{V^{(l_3)}_{q[\omega_0 t]}(t)}{L^{(l_3)}}\right). \end{aligned} \tag{21}$$

7.3 Results

A test case is considered where all four models have the same initial conditions, but at $t = 20$[s], the load resistance changes to $0.1\text{k}\Omega$, the load inductance changes to 10mH and the capacitance changes to 70μF. The comparison between the models is captured in Fig. 1–4 below.

The model responses are depicted with time-scale resolutions of 5 seconds, 50 milliseconds and 500 microseconds. We observe that at these time resolutions, the accuracies of μROm3, μROm2 and μROm1, respectively, are visible. This is consistent with the result in Table 1.

8 Conclusion

In this work, we developed a microgrid high-order model (μHOm) by using circuit-theoretic and control laws. We used singular perturbation techniques for model-order reduction of the μHOm, which allowed us to obtain three reduced-order models, μROm1, μROm2 and μROm3, with the time resolution of each reduced-model identified.

Table 2: System Parameters

	Parameter	s_1	s_2	$e_1 = \{1,3\}$	$e_2 = \{2,3\}$	l_3
Battery	$V_{DC}^{(s_j)}$	900V	900V	n/a	n/a	n/a
Three-Phase Inverter	$S^{(s_j)}$	10kVA	12kVA	n/a	n/a	n/a
	$V_{DQ}^{(s_j)}$	321.0265V	321.0265V	n/a	n/a	n/a
LCL filter	$r_0^{(s_j)}$	0.1Ω	0.15Ω	n/a	n/a	n/a
	$l_0^{(s_j)}$	1.35mH	1.5mH	n/a	n/a	n/a
	$r^{(s_j)}$	0.03Ω	0.04Ω	n/a	n/a	n/a
	$l^{(s_j)}$	0.35mH	0.33mH	n/a	n/a	n/a
	$\tilde{r}_0^{(s_j)}$	$15\text{m}\Omega$	$16\text{m}\Omega$	n/a	n/a	n/a
	$c^{(s_j)}$	50μF	60μF	n/a	n/a	n/a
Inner Current Control	$\kappa_{P\gamma}^{(s_j)}$	10.4479	10.4479	n/a	n/a	n/a
	$\kappa_{I\gamma}^{(s_j)}$	6.374×10^5	6.374×10^5	n/a	n/a	n/a
Outer Voltage Control	$\kappa_{P\phi}^{(s_j)}$	6.1825	6.1825	n/a	n/a	n/a
	$\kappa_{I\phi}^{(s_j)}$	1.364×10^4	1.364×10^4	n/a	n/a	n/a
Droop Control	$D_{\omega}^{(s_j)}$	13.2629	13.2629	n/a	n/a	n/a
	$D_{E}^{(s_j)}$	2.3368	2.3368	n/a	n/a	n/a
Network	$r^{(e_m)}$	n/a	n/a	0.35Ω	0.4Ω	n/a
	$l^{(e_m)}$	n/a	n/a	1.5mH	2mH	n/a
Load	$r^{(l_j)}$	n/a	n/a	n/a	n/a	$0.2\text{k}\Omega$
	$l^{(l_j)}$	n/a	n/a	n/a	n/a	11mH
	$c^{(l_j)}$	n/a	n/a	n/a	n/a	64μF

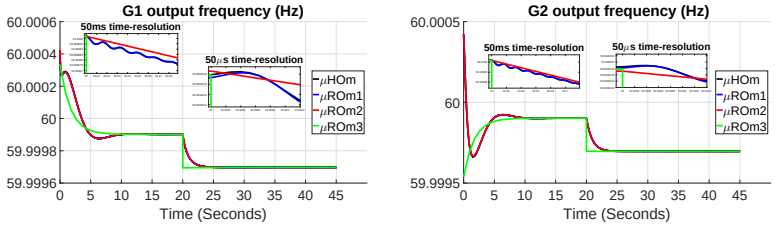

Fig. 1: Generator Output Frequency (Hz)

For a given test case, we compared the responses of all three models to that of the μHOm. Using the time resolutions to analyze each models response, we observed that the responses of μROm1, μROm2 and μROm3 track the response of the μHOm with errors $\mathbf{O}(\varepsilon_1)$, $\mathbf{O}(\varepsilon_2)$ and $\mathbf{O}(\varepsilon_3)$, respectively, where $\varepsilon_1 = 10^{-5}$, $\varepsilon_2 = 10^{-3}$ and $\varepsilon_3 = 10^{-1}$.

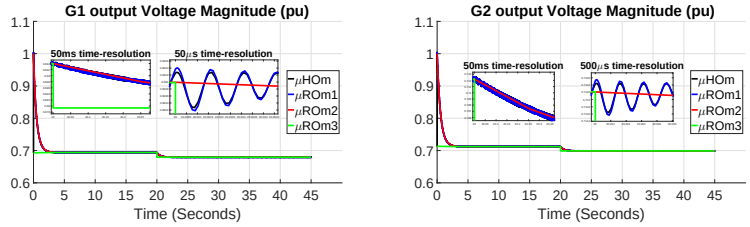

Fig. 2: Generator Output Voltage Magnitude (pu)

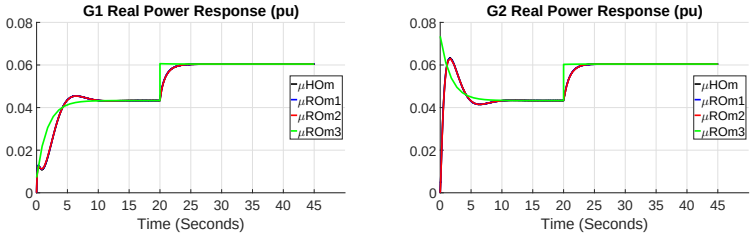

Fig. 3: Generator Output Real Power (pu)

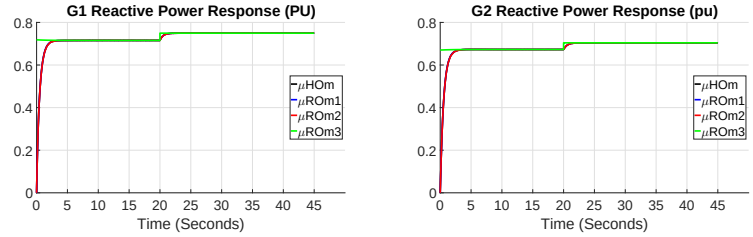

Fig. 4: Generator Output Reactive Power (pu)

References

[1] S. Anand and B. G. Fernandes. Reduced-order model and stability analysis of low-voltage dc microgrid. *IEEE Transactions on Industrial Electronics*, 60 (11):5040–5049, Nov. 2013.

[2] A.R. Bergen and V. Vittal. *Power Systems Analysis*. Prentice Hall, 2000.

[3] J. H. Chow. *Time-Scale Modeling of Dynamic Networks with Applications to Power Systems*. Springer-Verlag, 1982.

[4] F. Dörfler and F. Bullo. Synchronization and transient stability in power networks and non-uniform kuramoto oscillators. In *Proceedings of the 2010 American Control Conference*, pages 930–937, June 2010.

[5] K. Kodra, Ningfan Zhong, and Z. Gajić. Model order reduction of an islanded microgrid using singular perturbations. In *Proc. of American Control Conference, pp. 3650-3655, Chicago, IL, 2016*.

[6] P. Kokotović, H. K. Khalil, and J. O'Reilly. *Singular Perturbation Methods in Control: Analysis and Design*. Classics in Applied Mathematics. Society for Industrial and Applied Mathematics, 1986.

[7] P.C. Krause, O. Wasynczuk, S.D. Sudhoff, S. Pekarek, Institute of Electrical, and Electronics Engineers. *Analysis of Electric Machinery and Drive Systems*. IEEE Press Series on Power Engineering. Wiley, 2013.

[8] L. Luo and S. V. Dhople. Spatiotemporal model reduction of inverter-based islanded microgrids. *IEEE Transactions on Energy Conversion*, 29(4):823–832, Dec. 2014. ISSN 0885-8969.

[9] O. O. Ajala, A. D. Domínguez-García, and P. W. Sauer. A Hierarchy of Models for Inverter-Based Microgrids. Coordinated Science Laboratory Technical Report UILU-ENG-17-2201, University of Illinois at Urbana-Champaign, May 2017. URL http://hdl.handle.net/2142/96001.

[10] N. Pogaku, M. Prodanovic, and T. C. Green. Modeling, analysis and testing of autonomous operation of an inverter-based microgrid. *IEEE Transactions on Power Electronics*, 22(2):613–625, Mar. 2007.

[11] M. Rasheduzzaman, J. A. Mueller, and J. W. Kimball. Reduced-order small-signal model of microgrid systems. *IEEE Transactions on Sustainable Energy*, 6(4):1292–1305, Oct. 2015.

[12] P.W. Sauer and A. Pai. *Power System Dynamics and Stability*. Stipes Publishing L.L.C., 2006.

[13] J. Schiffer, D. Zonetti, R. Ortega, A. M. Stankovic, T. Sezi, and J. Raisch. Modeling of microgrids - from fundamental physics to phasors and voltage sources. *CoRR*, abs/1505.00136, May 2015.

[14] A. Yazdani and R. Iravani. *Voltage-Sourced Converters in Power Systems*. Wiley, Jan. 2010.